In presenting the dissertation as a partial fulfillment of the requirements for an advanced degree from the Georgia Institute of Technology, I agree that the Library of the Institution shall make it available for inspection and circulation in accordance with its regulations governing materials of this type. I agree that permission to copy from, or to publish from, this dissertation may be granted by the professor under whose direction it was written, or, in his absence, by the dean of the Graduate Division when such copying or publication is solely for scholarly purposes and does not involve potential financial gain. It is understood that any copying from, or publication of, this dissertation which involves potential financial gain will not be allowed without written permission.

AN INVESTIGATION OF THE STRENGTH OF ROCK

A THESIS

Presented to

The Faculty of the Graduate Division

by

Arnold Edward Schwartz

In Partial Fulfillment

of the Requirements for the Degree

Doctor of Philosophy

in the School of Civil Engineering

Georgia Institute of Technology

May, 1963

AN INVESTIGATION OF THE STRENGTH OF ROCK

Approved:

Date approved by Chairman: 5/20/63

DEDICATION

This thesis is dedicated to my wife for her patience and encouragement during these years of graduate study.

ACKNOWLEDGEMENTS

The author wishes to express his gratitude to Professor George F. Sowers for his advice and direction of this investigation; and to the members of the reading committee, Dr. A. B. Vesic and Dr. H. W. Straley, III, for their assistance in the preparation of this manuscript.

TABLE OF CONTENTS

TABLE OF CONTENTS (Continued)

LIST OF TABLES

LIST OF ILLUSTRATIONS

SUMMARY

Knowledge of the strength and physical properties of engineering materials aid in the design of more economical structures; consequently, they have been extensively investigated. However, the ultimate base of all structures, rock, has been somewhat neglected. The first attempt to determine the strength of rock under conditions imilar to its natural confinement began a little more than 60 years ago. Adams and Nicholson in 1901 applied axial loads to core samples of marble which were surrounded by tight fitting, steel cylinders. By 1911, von Kármán had improved this technique by introducing fluid pressure to provide controlled confinement. Griggs conducted triaxial tests on unjacketed specimens of several rocks in 1935. Rock testing procedures were reviewed in 1945 by Terzaghi who suggested that future testing should include controlled pore pressure in addition to the confining pressure. Tests of this nature were conducted by the U. S. Bureau of Reclamation during the 1950's, by Robinson in 1959, and by Serdengecti and Boozer in 1961. In all of these tests with pore pressures independently controlled, only rock specimens of relatively high porosities were used.

All investigators to date have agreed that an increase in confining pressure increases the strength of rock. However, no significant agreement has been reached regarding the behavior of rock under both confining and pore pressures. Neither the failure mechanism of rock, nor a criterion for failure have been established. The purpose of the present investigation is to resolve the differences brought forth by previous

studies and, in particular, to: (1) recommend a failure criterion, (2) evaluate strength components of rock, (3) express shear strength in terms of some fundamental parameters, and (4) examine the effect of pore pressures on strength.

Since experimental data for rock strength are still quite limited, more than 160 triaxial shear tests were conducted using four different rocks. Typical porous rocks, Indiana limestone and Pottsville sandstone, were tested under the following conditions: (1) dry, unconfined; (2) dry, confined; (3) wet, confined with zero pore pressure; and (4) saturated, confined with constant pore pressure. Rocks having relatively low porosities, Stone Mountain granite and Georgia marble, were tested (1) dry, unconfined; (2) dry, confined; and (3) saturated, confined with constant pore pressure. The confining pressures used in these tests ranged between zero and 10,000 psi. Pore pressures up to 5,000 psi were applied to the saturated samples with confining pressures always greater than or equal to the pore pressures. Each sample was separated from the confining fluid, hydraulic oil, by a vinyl plastic membrane. Distilled, de-aired water was used as the interstitial fluid in all the pore pressure tests.

From the triaxial tests, stress - strain curves were obtained which all have initial straight line parts. For the sandstone and granite, these curves indicate a peak value of deviator stress. Fracture occurs almost immediately thereafter. The same is true for the limestone and marble when tested under confining pressures less than 5,000 psi. With confining pressures greater than 5,000 psi, the stress - strain curves for the marble and limestone do not reach a peak value; instead, stress continues to increase with additional strain. All of the rocks tested

show an increase in strength with a corresponding increase in confining pressure.

The test data are also presented in terms of Mohr's circles for the failure stresses. For the rocks which fractured in a brittle manner, failure stress was defined as the maximum value of deviator stress obtained. Deviator stress values continually increased for the rocks failing in a ductile manner; however, this increase was linear with strain after failure. The stress value at the beginning of this straight-line portion of the stress - strain curve was used to define the deviator stress at failure. (This is referred to as the Jeffrey criterion.)

Envelopes for the stress circles have been constructed which have two distinct portions, the initial portion being non-linear, the remainder linear. Tension tests were also conducted for each rock in order to determine more accurately the shear axis intercept value for each envelope. The angles of failure were calculated from the Mohr envelopes and compared to the angle measured for each sample. These angles agreed closely for most specimens except those tested under confining pressures less than 3,000 psi. For these samples, the measured angle was less than that predicted by the Mohr criterion.

Microscopic studies were made to determine the condition of the failure surfaces. Samples tested with confining pressures less than 3,000 psi had failure surfaces which were irregular and free of loose particles. A similar surface was observed in the tension tests. For specimens tested under confining pressures greater than 3,000 psi, the failure surfaces appeared slickensided and contained granulated crystals of variable size. A combination of these failure surfaces was noted in most samples tested under confining pressures between 2,000 and 4,000 psi.

The maximum deviator stress for the saturated samples of limestone and sandstone under constant pore pressure was nearly equal to the dry strength of these rocks tested with confining pressures equal to the "effective confining pressure" applied to the saturated samples. The granite and marble, when tested under constant pore pressure, had almost the same strength regardless of the magnitude of the applied pore pressures.

The conclusions reached in this investigation are:

(1) The Jeffrey criterion is suitable for the determination of maximum deviator stress.

(2) Rock fails by either splitting, shear, or pseudo-shear.

(3) Failure of rock is brittle or ductile depending upon the amount of confining pressure.

(4) Shear failure will occur in rock if confining pressures are sufficient to prevent splitting.

(5) The angle of slip for shear failure is closely predicted by the Mohr criterion.

(6) Shear strength of rock may be considered the sum of cohesion, internal friction, and "fracture interference."

(7) Fracture interference appears to be a unique function of normal stress for all the rocks tested.

(8) The concept of "effective confining pressure" is not universally valid.

CHAPTER I

INTRODUCTION

Statement of the Problem

Among the least investigated engineering materials are rocks. Although great effort has been expended to minimize the quantity of material required in engineering structures by defining thoroughly the structural behavior of the component materials for nearly all conceivable stress conditions, the ultimate base of all structures, rock, has been somewhat neglected. The reason for this neglect has been partly in the fact that loads placed on foundation rock usually have been of such a small magnitude compared to the strength that failure in the rock was almost unheard of. However, there are circumstances in which the strength and stress conditions of rock have been considered for quite sometime. Probably the most critical of these is tunneling in rock. Many examples of tunneling in rock may be found on railways and highways in mountainous regions and also at dam sites where diversion tunnels are cut into the rock. For arch dams the strength of the supporting canyon walls is of great concern and its accurate evaluation is mandatory. The mining industry with its complex of tunnels and shafts into the depths of the earth has suffered many disasters because of rock failure. Landslides in open pit mines and along roadways constantly present an economic burden to both industry and taxpayer. The petroleum industry has also become increasingly concerned about the behavior of rock under its natural confinement in their search for more economical drilling methods.

The development of nuclear facilities uncovered the problem of radioactive waste disposal - one solution is the deposition of waste material in deep openings hollowed out in rock. The military threat of the atomic age also displayed the need for construction of deep vaults in solid rock to preserve the records of civilization and perhaps civilization itself.

The necessity of providing engineering structures in the earth's crust brings up the question - what is the behavior of rock under stress?

CHAPTER II

REVIEW OF LITERATURE

History of Strength Testing of Rock

The problem of determining the strength of rock under conditions similar to those deep in the earth's crust can be traced to the beginning of the 20th century. Methods of testing rock prior to this time consisted of merely an unconfined compression or direct shear of rock samples so that the mechanism of failure remained purely a matter of speculation. Investigators began to search for a laboratory method of duplicating the in situ confinement of deeply buried rock strata.

The first solution to this problem was proposed by Adams and Nicholson, 1901 (1), who produced the needed confinement by surrounding cylindrical marble samples with a tight fitting, thick walled, steel jacket. Pistons at each end of the rock core placed it in axial compression. The longitudinal axial strain exerted by the load pistons caused a strain of opposite sense in the radial direction commonly referred to as the Poisson effect. Since the heavy steel jacket restricted the circumferential expansion of the rock, a pressure at right angles to the axial load was created at the mutual boundary of rock and steel.

Further studies (14) were carried out using steel-jacketed cylinders at later dates by Adams, 1910, 1912; Adams and Bancroft, 1917; Adams and Coker, 1910; King, 1912, 1917. The common result of these investigations as described by Handin, 1957 (16), was the conclusion that the ultimate strength and ductility of rock increases with the amount of

confinement. No exact relationship between increased strength and confining pressure could be established on the basis of these tests because, according to Griggs, 1936 (13), p. 543:

> (1) It is impossible to measure exactly the confining pressure because of the friction between the jacket and the specimen;
> (2) since the confining pressure depends on the amount of bulging of the jacket it increases as the deformation of the specimen increases, hence the confining pressure is sensibly zero at the moment of beginning the deformation;
> (3) by this method of confining the specimen is not free to fracture by major shear or tension fractures, since a fracture would have to tear through the walls of the steel jacket.

These inadequacies inherent with steel-jacketed testing were recognized by von Kármán, 1911 (20), who conducted the first useful triaxial tests. The apparatus used by von Kármán consisted of a confining cylinder large enough so that the rock sample could be surrounded by a liquid. Two pistons passed through upper and lower seals at opposite ends of the confining cylinder. The upper piston was used to apply the axial load to the rock core. The lower piston was forced upward by a hydraulic ram into a chamber just below the support for the bottom of the core sample. A hole passed through the sample support leading from the lower chamber to the sample chamber to provide the confining pressure. The outstanding features of von Kármán's test procedure were: (1) the axial stress on the rock sample and the confining pressure could be applied independently and accurately measured, (2) the confining pressure remained constant throughout the test, and (3) no friction was created between the sample and its lateral confinement, and (4) deformation along slip planes in the sample was not inhibited.

Aside from this outstanding development of testing apparatus, von Kármán also discovered the merit of placing an impermeable membrane around

the specimens to separate the pore spaces in the rock from the confining fluid. Unfortunately, suitable materials for this purpose had not yet been developed at that time; therefore, the sample was encased in brass tubing with thin walls to minimize its contribution to the strength of the sample.

Test results on two rocks, Carrara marble and red sandstone, were reported by von Kármán. A relationship between confining pressure and rock strength was described for the first time. From this data stress-strain curves were plotted for rocks deformed under pressures varying from zero to several thousand pounds per square inch (marble-up to 49,000 psi, sandstone - up to 37,000 psi). Von Kármán presented this test data in terms of Mohr's stress circles (see Appendix) for which he constructed a curvilinear envelope. His conclusions were: (1) the strength of rock is greatly enhanced by lateral confinement, and (2) Mohr's theory affords a suitable representation of the triaxial test data for rock samples.

Further investigation was carried out by Böker, 1915 (6), who performed extension tests on rock ($\sigma_1 = \sigma_2 > \sigma_3$). Later tests by Roš and Eichinger, 1928 (28), confirmed von Kármán's observations.

Griggs, 1936 (13), under the supervision of Bridgman, conducted a series of high pressure triaxial tests on Solenhofen limestone, marble and quartz. The apparatus and methods of high pressure followed very closely the techniques developed by Bridgman, 1931 (9). With the exception of the device used to measure the intensity of the confining pressure, the triaxial apparatus used in these tests was almost identical to that designed by von Kármán. Griggs, however, failed to use a jacket around the rock samples in the majority of his tests. Nadai, (25) p. 244 notes that:

> Griggs . . . exposed most of the cylindrical specimens of very porous rocks such as limestone . . . to the action of the pressure fluid (kerosene) which was permitted to penetrate in the crevices of the material under the high hydrostatic pressures. His test results were therefore obscured through this secondary effect.

Griggs (13), p. 544 and p. 556, had the following comment on his own testing procedure:

> These conditions of testing (confining fluid around unjacketed samples) give values for strength, show changes in the mode of fracture, and permit the study of plasticity in specimens which, by direct comparison with laboratory experiments at atmospheric pressure, show the changes in physical properties caused by the confining pressure. Conditions in the earth's crust are not simulated, however, since any unit of rock in nature is surrounded by other rock. It seems certain that this surrounding rock presents more resistance to fracture of the unit under consideration than would a surrounding liquid. It is equally certain that the surrounding rock does not present so much resistance to fracture as Adams' steel jacket, since the strength of the surrounding rock is not greater than that of the unit considered . . . . It may be that better accord with Adams's results will be reached when more experiments are performed with a confining jacket to keep the liquid out of the pore spaces (of the rock).

Two types of failure were observed by Griggs, shear and tension. The shear surfaces he observed gave evidence of fracturing and powdering of the crystals. These surfaces appeared lighter in color than the surface of a fresh break of the rock sample, were commonly slickensided, and showed granulation of the crystals. The slip planes developed by the shear failure were always at an angle with the direction of the axial load. The tension fracture occurred by splitting parallel to the direction of the compression. No granulation appeared on this surface.

The tension failure, or splitting phenomenon, was explained by Griggs as the result of the formation of wedge shaped failure planes at the top and bottom of the sample. If confining pressures were of low magnitude these wedges caused the sample to split because of the tension developed between the grains at the point of the wedge. Careful

observations with high speed movie film made by Griggs confirmed the hypothesis that the slip or shear surfaces appear prior to the tension fracture. Terzaghi, 1945 (34), presented a similar theory for splitting failure attributing the tension between two grains to the wedging action of a third grain trying to push its way between them. Griggs further observed that as confining pressures increased the splitting failure would be prevented, assuming the liquid had no access to the wedge point, and shear fracture would predominate.

Soon after the concept of "effective stress" was introduced in soil shear strength (33), attention was turned to the corresponding problem in rocks. Terzaghi (34) commented that the stress conditions for the failure of rocks, subjected to a neutral pressure combined with a confining pressure, remain a matter of opinion until tests are conducted in which these pressures are controlled independently.

A triaxial cell capable of sustaining pore and confining pressures independently, has been described by Blanks and McHenry, 1945 (5). A very large piece of triaxial equipment was built for the U. S. Bureau of Reclamation, Denver Laboratories, which measured over six feet high and three and one-half feet in diameter. Six by twelve inch rock cores could be tested under confining pressures up to 125,000 psi.

The Bureau of Reclamation was authorized in 1950 to initiate an extensive testing program to study in detail the physical properties of a large variety of foundation rocks (4). All triaxial specimens were jacketed with a rubber membrane. Test data was presented in terms of Mohr's stress circles and approximated by straight line envelopes. Primarily the Bureau was concerned with triaxial characteristics of rocks

under confinement similar to that expected in their foundation problems. As a result, their lateral pressures rarely exceeded 2000 psi in their tests and no attempt was made to define the Mohr envelope beyond the straight line approximation. Balmer, 1953 (4), compiled the results of this program and placed "confidence limits" on this parametric representation of the Mohr envelope. No mention of pore pressure tests was made in his report.

Additional data on rock strength was obtained by Robertson, 1955 (26), who tested Solenhofen limestone, fossiliferous limestone, shaly limestone, marble, granite, diabase, quartzite, slate, soapstone, verde antique, and sandstone. He used three experimental procedures: (1) compression of solid cylinders, (2) crushing of hollow cylinders, and (3) punching of disks. The triaxial tests were conducted using rubber jacketed specimens under confining pressures from one to 60,000 psi. Robertson observed plastic flow in the limestone and marble samples which was absent in the silicate rocks. He concluded that the maximum shear stress theory could be used to predict the yield point in the limestones but only found a rough empirical criterion for the silicate rocks. Independent control of pore pressure was not possible with Robertson's test cell, therefore, only dry samples were used.

Triaxial tests using moderate confining pressures (0 - 15000 psi) were conducted by Bredthauer, 1957 (8), on a variety of marbles, limestones, and sandstones. Rock specimens jacketed with plastic tubing were tested in an air-dry condition. When Bredthaur calculated the values of differential stress, he assumed the volume of the rock sample to remain constant (equivalent to assuming a Poisson's ratio of 0.5). The

measured angles of fracture he states, may or may not represent shear planes since failure may occur as a combination of shear and tension. This is the pseudo-shear failure mentioned by Terzaghi, 1945 (34). No other conclusions regarding the mechanism of rock fracture or compatibility of failure theories were made by Robertson.

Handin and Hager, 1957 (16), reported triaxial studies on limestones, dolomites, sandstone, shales, anhydrite, quartzite, siltstone, and slate. Their test cell was patterned after Griggs' and they likewise used kerosene for a confining fluid. The samples were one inch long and 1/2 inch diameter, jacketed in thin wall copper tubes. Handin also assumed no volume change in order to calculate the "true" deviator stress. The maximum load supported by the rock sample was used as a measure of the ultimate strength. For rock samples which did not rupture but failed plastically, strain was stopped at 30 percent because of limiting conditions in the triaxial apparatus. Handin concluded that the Coulomb - Mohr theory is not valid for all states of stress but can be fitted to the largest principal stress circles resulting from the triaxial compression tests. In contrast to von Kármán (20), Handin found the predicted angles of the failure planes to be different from the observed angles. Although no pore pressure tests were reported in this paper (16) Handin speculated, based on the results of tests on unjacketed porous rock, that the strength of rock will depend on the "effective confining pressure" which is the difference between the confining and pore pressures. A similar observation was made by Terzaghi (34).

One of the few applications of triaxial testing of rock to foundation design was made by Moye, 1958 (24), who tested gneiss and granite

under confining pressures of 0 - 15000 psi. No mention is made of the type of membrane used, if any, or pore pressure studies.

An extensive series of triaxial tests with controlled pore pressures has been conducted by Robinson, 1959 (27), who studied the strength of limestones, sandstones and shale. His results present evidence that the strength of porous rocks is a function of the "effective confining pressure." Several tests were made on saturated samples with the confining and pore pressures equal. A nearly constant value of shear strength was recorded for pressure ranges of 0 - 10000 psi. A noted exception to this statement was the slightly lower strength values for the limestones at low confining pressures, in particular, the unconfined sample with zero pore pressure. During the tests Robinson detected a change in pore volume which decreased slightly during initial deformation, and increased at the point of yielding and thereafter. In accordance with von Kármán, Robinson illustrated his test results by drawing Mohr's stress circles for the principal stresses at failure and enclosed these circles with a curvilinear envelope.

The results of a petrographic analysis conducted on a shear surface of Indiana Limestone are described by Robinson (27), p. 195:

> . . . the thin section analysis of the Indiana Limestone revealed that the crystals twin and then fail by a shear fracture. In other words, even when a large differential pressure is applied to the rock, the force-deformation diagram indicates a material which is truly plastic in nature. Although the crystals do exhibit a plastic deformation by twinning, there is also brittle fracture occurring through the grains. It is conceivable that, as the pore pressure is decreased from the confining pressure, a greater number of shear planes transverse the core, and the shear planes become shorter.

His conclusions may be summarized:

(1) Malleable or brittle failure may occur in sedimentary rocks

depending on the difference between pore and confining pressures, (2)brittle failure always occurs when these pressures are equal and mode of failure changes from brittle to malleable depending on pressure level and nature of the rock, (3) yield strengths of rocks increase only slightly as confining and pore pressures are increased but maintained equal.

Serdengecti and Boozer, 1961 (31), have tested rock specimens under the influence of an additional variable, temperature. The outstanding features of their cell are: (1) confining and pore pressures may be varied from 0 - 20,000 psi, (2) strain rate of the axial load range from 0.001 to 100 percent per second, and (3) temperature may be raised from room to 300° F. A rubber jacket is used to separate the 1-1/2 inch by 3/4 inch core sample from the confining fluid. The maximum deviator stress* which may be applied to the rock specimens is 75,000 psi.

They conclude that of the effects of interstitial fluids on the strength of rock have "demonstrated conclusively that the effective pressure concept was equally valid at all strain rates and temperatures" (31), p. 13. This view has not been substantiated by others (38). They have also shown the marked influence of strain rate and temperature on samples of Berea sandstone, Solenhofen limestone, and Pala gabbro. As strain rate was increased the axial compressive stress required for rock fracture increased and the type of failure changed from ductile to brittle. The effects on strength and ductility observed when strain rate was held constant and temperature increased was qualitatively equivalent to decreasing the strain rate.

---

*Deviator stress as used throughout this paper refers to the difference in principal stresses, that is, $(\sigma_1 - \sigma_3)$.

It is interesting to note that Serdengecti and Boozer also use the assumption that no volume change resulted when the specimens were tested in order to calculate "true" differential stresses.

Serata, 1961 (30), used a test cell nearly identical to that of Adams, 1901 (1); thus the present author again refers to the comments by Griggs, 1936 (13) regarding this procedure.

Hypothesis on the Strength of Rock

Since the early tests of Adams the shear strength of rock has captured the interest of many authors. Although a number of these have not personally conducted laboratory tests, their comments and ideas have been of great interest.

There has been much discussion about the selection of the maximum deviator stress for materials which do not have a distinct yield point or peak value. An excellent definition of material strength was given by Jeffreys, 1924 (19), as "the critical stress difference above which the rate of change of shape does not decrease when the time of application of the stress increases".

Terzaghi, 1945 (34), outlined a procedure by which a successful investigation of rock strength might be carried out. Essentially his procedure directed that rock samples be tested under the following conditions: (1) dry, unconfined; (2) dry, confined; (3) saturated, unconfined; and (4) saturated, confined where pore and confining pressures could be controlled independently.

Rock failure, according to Terzaghi (34), may be classified as splitting, shear, or pseudo-shear depending on the inclination of the failure planes. Splitting may be recognized by cracks appearing parallel

to the direction of the axial load which seems to indicate that the bonds between grains fail by tension. The tension between adjacent grains is caused by the wedging action of an intermediate grain. Shear failure occurs when grains and bonds alike are displaced along a glide plane whereas pseudo-shear failure represents a combination of shear and tension fracture.

Terzaghi (34) further states that there are several discrepancies between Mohr's theory (of failure) and reality. However, he says, this theory gives an approximate conception of stress conditions at failure for quasi-isotropic materials such as rocks. With little or no confining pressure, the position of the surfaces of failure may be very different from what Mohr's theory would lead us to expect. With increasing confining pressures, the errors become less and less important because the type of failure approaches more and more that of a pure shear fracture. The importance of the deviation of the type of failure from one due to pure shear can be ascertained by comparing the angle of the real failure surface with the slope angle predicted by Mohr's envelope.

Nadai, 1950 (25), in Chapter 16, discusses the conditions of failure for various materials. "The cleavage (Terzaghi's tension) and shear fractures in brittle polycrystalline materials (rocks) under a moderately large mean stress $(\sigma_1 + \sigma_2 + \sigma_3)/3$ seem to follow the conditions specified by the Mohr theory," (25) p. 230. The basic difference between the Mohr and von Mises criteria is explained by Nadai (25) p. 230:

> After recalling that the limiting condition of yielding $f_1(\sigma_1,\sigma_2,\sigma_3) = 0$ may be represented by a surface of yielding in a system of rectangular coordinates $\sigma_1,\sigma_2,\sigma_3$ we may add that the theories of flow based on conditions of slip, the Mohr, the maximum shearing stress, or the Guest theories, in which the hypothesis is made that the value of the intermediate principal stress σ_2 (when $\sigma_1 > \sigma_2 > \sigma_3$) has no influence on

> the condition of yielding, lead to six distinct conditions of flow (in which, however, always one of the three principal stresses does not appear) and are represented consequently in a $\sigma_1,\sigma_2,\sigma_3$ system of coordinates by surfaces having six sides. The discontinuity inherent in the form in which the conditions of slip and of yielding were assumed by Mohr leading to surfaces of yielding with six edges was eliminated by von Mises (22) when he proposed replacing the regular hexagonal prism representing the maximum shearing stress theory by the surface of the circumscribed straight circular cylinder expressing also the conditions of a constant octahedral shearing stress.

Topping, 1955 (35), reviewed failure theories and their applicability to rock strength. He recalls Schleicher's (29) suggestion that the limiting octahedral shearing stress be expressed as a function of the mean principal stress, $1/3(\sigma_1 + \sigma_2 + \sigma_3)$. This theory, then, has the same relationship to the von Mises (22, 17) criterion as the Mohr theory has to maximum shear stress theory.

Another review of failure criteria is given by Silverman, 1957 (32), who advocated the use of Mohr's theory for fracture and flow of rock like materials.

A comparison of the Mohr and Griffith criteria was given by Clausing, 1959 (11). In his opinion Griffith's theory and experimental results refute Mohr's concept of failure.

Borowicka, 1962 (7), made a comparison of the mechanical properties of soils and rocks. He showed that for crystalline solids a basic distinction must be made between metals and nonmetallic brittle materials. The shear strength of metals, which have a dense structure, is due to true cohesion whereas the strength properties of nonmetallic brittle materials are derived from numerous internal surfaces and are therefore regarded as heterogeneous bodies. They possess a grain skeleton in which internal friction is effective whereas true cohesion is simulated by an internal skeleton pressure existing in the grain skeleton.

Summary of the Present State of Knowledge

Studies and experiments concerning the strength of rock have indicated the following:

(1) All investigators mentioned in this chapter agree that hydrostatic confining pressures increase the strength of rock.

(2) Many, such as Terzaghi, Handin, Griggs, Robinson, Serdengecti, and Boozer have stated that interstitial, or pore, pressures cause a significant reduction in strength. Robinson, Serdengecti, and Boozer proposed that this reduced strength is predicted by calculating the "effective confining pressure" surrounding the rock sample. According to them, "effective confining pressure" is simply the numerical difference between the external lateral confinement and the pore pressure. However, these investigators have only tested rock of high porosity in which the pore and confining pressures were independently controlled. Terzaghi, on the other hand, has suggested that the "boundary porosity" of unjacketed rock cores has the most influence on the strength of rock which is tested under both lateral and interstitial pressures.

(3) Only a few authors have discussed the failure mechanism in rock. Griggs and Terzaghi have both offered that rock fails by either tension between grains, shear, or psuedo-shear; the latter mode is a combination of the first two.

(4) Most researchers, von Kármán, Böker, Robinson, Serata, Borowicka, and several others have represented their data for rock tests by means of Mohr stress circles and rupture envelope. Terzaghi pointed out that this method of representation was satisfactory and the errors involved become very small as confining pressures become greater. Topping, however,

prefers the von Mises hypothesis as revised by Schleicher so that the influence of intermediate principal stresses on rock strength is included. Clausing, on the other hand, was in favor of Griffith's theory of fracture to explain the behavior of rock under stress.

(5) A serious difficulty in comparing test data is the lack of a suitable failure criterion. Robinson has used the offset method to determine the failure stress of his rock specimens. Von Kármán, Griggs, and Handin used the maximum stress reached during their tests regardless of the shape of the stress - strain curves for their samples. Topping and Jeffreys proposed that the ductility of the rock must be considered when determining the failure stress.

Thus, no significant agreement has been reached regarding the behavior of rock under both confining and pore pressures, the failure mechanism, or a suitable failure criterion.

CHAPTER III

PURPOSE OF THE RESEARCH

The purpose of this investigation is to study the phenomena of rock failure, and to resolve the discrepancies of previous research.

Failure Criterion

When examining the stress - strain curves for a given material it is sometimes difficult to determine the stress and strain values at which failure occurred. Therefore, before a successful investigation of how a material fails can be made, a definition or criterion of failure must be established.

Nature of Shear Strength

The primary concern in predicting the behavior of a material under a given stress is to be able to correctly evaluate its ability to sustain load without rupture - its strength. Consider a cubical element in a mass subjected to a loading. It has been shown by Mohr (23) that when this element is rotated the normal stresses on each face reach a maximum, intermediate, and minimum value and at the same instant, the shear stresses disappear. The stresses occurring at this instant are called the principal stresses. These normal stresses are sometimes more conveniently expressed in terms of the sum of a hydrostatic, or mean principal stress, and a deviator stress. It is not difficult to conceive that the state of stress in a rock mass would be one primarily where the principal stresses were of a compressive nature. Applied loads to the

rock mass would constitute then the application of a deviator stress of known direction.

In the study of crystalline materials two types of failure have been observed, cleavage and shear. Cleavage may be described as the pulling apart of particles which is resisted only by molecular bonds, and is therefore associated with the tensile strength of a material. Shear failure, on the other hand, is a result of a grain or particle distortion so that eventually one grain is forced to slide over another. Since the loads applied to rock are usually compressive, shear failure is most likely as these loads approach the strength capacity of the supporting media. Thus, the nature of the shear strength is examined in light of the contributing factors, in a qualitative sense, of which it is a function.

Mathematical Representation

In soil mechanics two shear strength parameters, cohesion and internal friction, have been found useful in describing the shear strength of soil under a given state of stress. Although it is not expected to explain the complex nature of crystalline solids such as rock in terms of these simplified parameters, they provide, along with additional considerations, a first insight into the components of shear strength for rock.

Pore Pressure Effects

Nearly all rocks contain an interstitial fluid in their pore cavities. This fluid may be static, but most often it is found to be flowing and does much to alter the surrounding rock both chemically and physically. Under a multitude of circumstances this fluid, most commonly water, is subjected to a wide range of pressures. A main objective of the

research is to evaluate the effect of pore pressure on the strength of rock. To obtain a clear evaluation of this effect, water was used as the interstitial fluid in the tests and is placed under a constant pressure so that test conditions are as near to those in situ as possible.

Purpose of this Investigation

In this study the author proposes to:

(1) select a suitable failure criterion for both brittle and ductile failure,

(2) examine the failure modes of rock samples tested under triaxial compression,

(3) present a parametric equation to represent the failure condition in rock, and

(4) compare the effect of interstitial pressures on the strength of porous and non-porous rocks.

CHAPTER IV

INSTRUMENTATION AND EQUIPMENT

The Triaxial Cell

A special triaxial cell was designed and built at the Georgia Institute of Technology to test the rock samples under lateral pressures from zero to 10000 psi and pore pressures from zero to 5000 psi. The base of the cell and the load piston were designed for a maximum load of 50,000 pounds or a maximum deviator stress of 73,000 psi under maximum lateral pressure.

The pressure cell was constructed of bearing bronze, high strength steel, and stainless steel. The base of the cell was made of the bearing bronze eight inches in diameter, and contained the ports for the lateral confining pressure and pore pressure. The center of the base was fitted with a high strength steel pedestal to act as a base for the rock samples. A cylinder of high strength steel was threaded onto the base and the connection sealed by one Buna-N O-ring. The upper seal of the cell was provided by a bronze packing gland threaded into the top of the cylinder and sealed in the same manner as the base. The center of the packing gland contained a movable piston of stainless steel sealed by four O-rings, two Teflon and two Buna-N. The piston contacted the upper end of the rock sample and was used to apply the vertical loading. The sample was placed between two small loading blocks of stainless steel, 7/8 inch in diameter, flat on the side in contact with the sample and spherical on the opposite sides which were matched to spherical depressions in the base and in the

piston. This feature allowed for slight misallignments incurred during sample preparation. A valve was located at the top of the cylinder to allow air to escape as the cell was being filled with hydraulic fluid through the entry port in the base. The pressure cell is illustrated in Figures 1 and 2.

The Pressure Accumulator

A pressure maintaining device to supply constant pore and lateral pressure was constructed on a movable framework fitted with locking swivel castors (see Figure 3). Three pressure units were installed: one each for pore pressure, lateral pressure, and vertical load. Each unit consisted of a pressure line equipped with an accumulator to recover losses of pressure and compensate for leakage. The accumulator also absorbed excess fluid to eliminate pressure surges. To perform the pressure compensation a cylinder and piston with an O-ring seal were installed on each pressure line. The capacity of each cylinder was approximately 50 cubic centimeters. As pressure was lost in the system a yoke pulled the piston into the cylinder to replace the lost fluid. The yoke was activated by a set of three pulleys connected by a common shaft and rigidly fastened to each other. The center pully was 15 inches in diameter and was in a 19.6:1 ratio with the two smaller outside pulleys. Stainless steel, high strength cables were connected to the yoke and passed through the two small pulleys. Another cable was placed around the large pully and attached to a weight hanger. The cross-sectional area of the piston was 0.196 square inches, thus a one pound weight placed on the weight hander would produce a pressure of 100 psi in the closed system. The

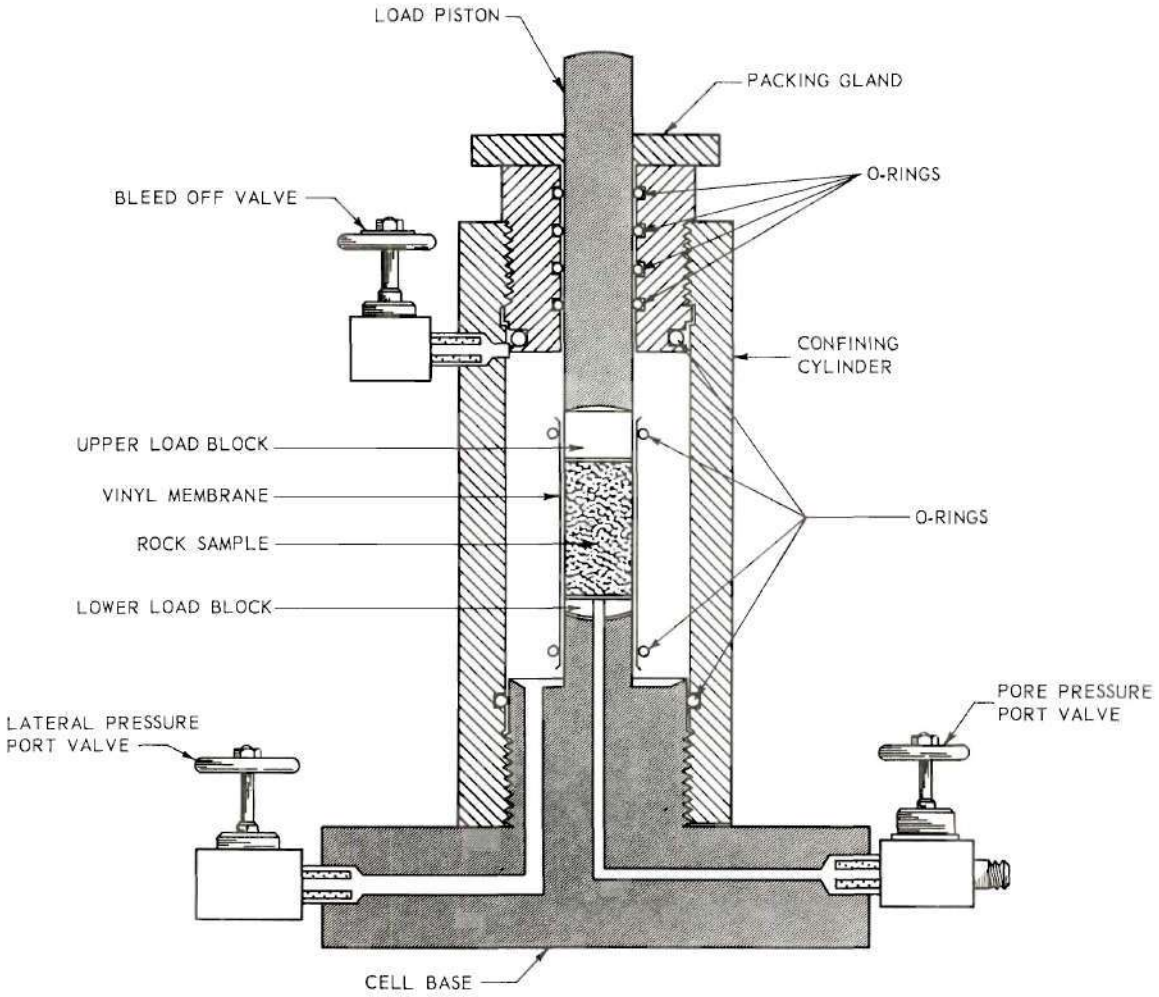

Figure 1. Cross-section of the Triaxial Cell.

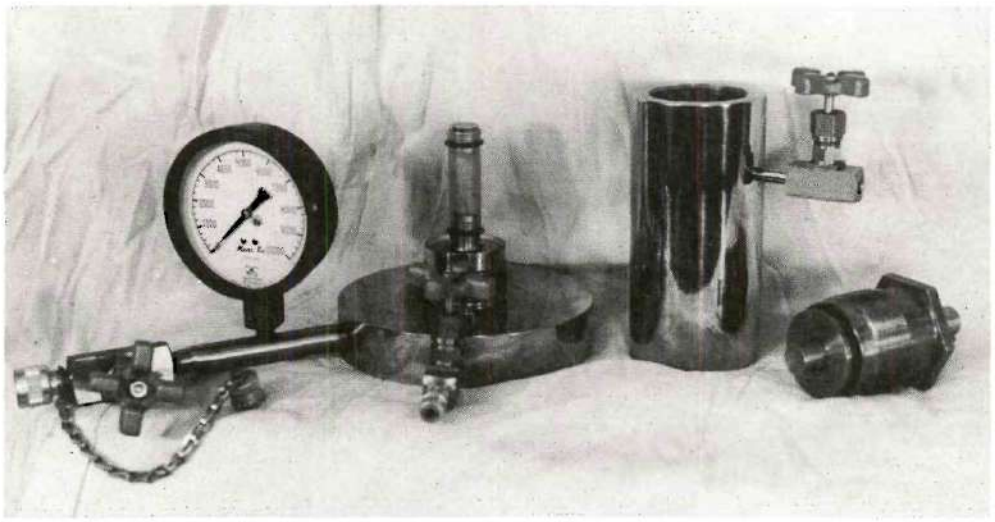

Figure 2. The Triaxial Cell.

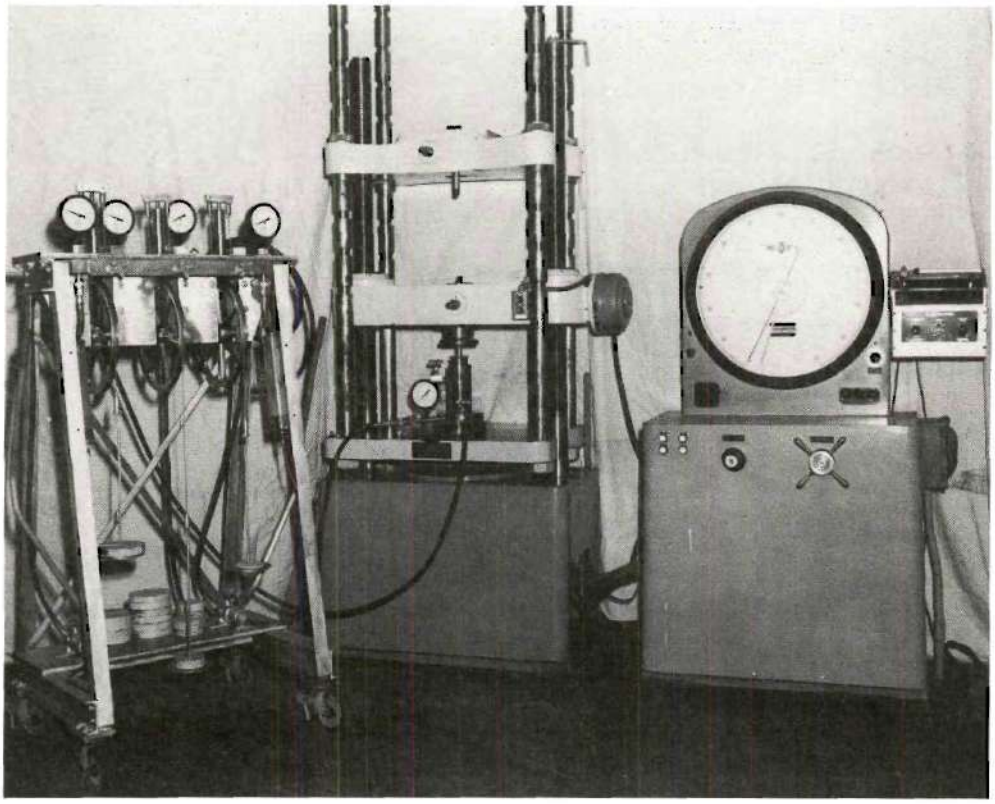

Figure 3. Trixial Cell, Accumulator, and Testing Machine.

accumulator was capable of maintaining a desired pressure within two percent over an extended period of time.

Loading Machines

Two loading machines were employed in the triaxial shear tests. For loads up to 20,000 pounds a constant strain mechanically driven machine was used at deformation rates of 0.01 inches per minute. For loads exceeding this capacity a hydraulic machine was used with the deformation rate controlled manually from approximately 0.005 inches per minute to 0.02 inches per minute for rocks with higher strain capacities. The test set up using the hydraulic machine is shown in Figure 5.

Measurement of Sample Deformation

A micrometer dial indicator having divisions of 0.0001 inches was used to record the sample deformation. Since the dial indicator was placed between the load table and the crosshead of the testing machine this measurement included not only the deformation of the rock sample but also the deformation of the components of the triaxial cell in contact with the rock sample. Therefore, the deformation of the steel load piston above the sample and that of the steel pedestal below the sample had to be subtracted from the total deformation reading. The deformation of the base of the triaxial cell was considered negligible since its area was many times that of the sample. The corrected deformation was then used to calculate the strain in the rock samples.

CHAPTER V

PROCEDURE

Description of the Rock Samples

Four rocks were investigated, two porous, and two non-porous. The samples consisted of Indiana limestone, Pottsville sandstone from Alabama, Stone Mountain granite, and Georgia marble.

Indiana Limestone

Indiana limestone is generally referred to as oolitic limestone because of the shape of the grains which resemble fish eggs. The limestone sample used in the tests was light buff in color which indicates its source to be from the upper part of the stratum. Deeper horizons are grey in color which indicates that the light color is probably due to oxidation of organic material. It would be well to quote Anderegg (2), p. 11, on the description of this material:

> Indiana limestone is of the type known as "free stone," working almost equally well in any direction. The strength parallel to the grain is almost as great as that perpendicular to the grain. Compressive strength . . . averages from 6000 psi to 7000 psi, being slightly greater for dry than for wet stone.

The term "free stone" comes from Old French franche pere which, literally translated, means excellent stone. As used technically the term refers to stone, especially sandstone or limestone, which can be easily cut without splintering (37).

Stone Mountain Granite

Stone Mountain granite is described by Watson (22), pp. 114, 116:

> Macroscopically, the rock is an even-textured, medium-grained, light grey, biotite bearing muscovite granite . . . .

The component minerals, quartz, feldspar, and the micas, muscovite and biotite are readily recognized by the unaided eye. Muscovite greatly predominates over the biotite in the hand speciman.

Microscopically, the rock is a medium-grained, allotrimorphic-granular granite, composed of an aggregate of complexly interlocking quartz and feldspar grains, with numerous grouped plates and shreds of muscovite and biotite.

Pottsville Sandstone

The Pottsville sandstone sample was obtained from a deep quary; appears uniform in color and unweathered. Chemically the stone is nearly pure silica. A cross-section shows that the rock consists of quartz crystals in contact with each other with small amounts of silica cement present at the points of contact. The quartz crystals appear uniformly clear and colorless, the entire sample, however, has a buff color due to a small amount of limonite (1-3 percent).

Georgia Marble

The Georgia marble is white and consists of nearly pure calcite. The marble sample is extremely dense, with a unit weight of 168 pounds per cubic foot. No pore spaces were visible under the microscope; the porosity was only three percent. Cleavage planes were clearly defined on the cross-section of the core samples.

A summary of the physical properties of all the rocks used in the triaxial tests is given in Table 1.

Table 1. Physical Properties of the Rocks Used in the Triaxial Tests

Type Rock	Sp. G.	Void Ratio	Density (pcf)	Average Unconfined Strength - psi
Indiana Limestone	2.705	0.240	137	6000
Pottsville Sandstone	2.64	0.163	142	9000
Stone Mountain Granite	2.66	0.022	163	4000
Georgia Marble	2.76	0.028	168	12000

Preparation of the Core Samples

Preparation of the rock samples was accomplished by using conventional machine tools which had been modified for the use of rock cutting and rock coring apparatus. A twelve inch diamond tooth circular saw was used to trim the rock specimens to suitable size and shape for coring. Two parallel faces were cut, producing a slab approximately two inches thick. In the sedimentary rocks these faces were cut parallel to the stratification so that the test core would be oriented in its natural position when placed in the triaxial test cell. A diamond impregnated coring bit, 7/8 inch inside diameter and one inch outside diameter, was used to produce a core sample from the previously prepared slabs. The coring bit was attached to a water head and was driven by a conventional drill press. Also adapted to the drill press was a three-hundred grit grinding wheel which was used to polish the ends of the core samples. A wooden jig made of oak held the sample during polishing. The oak jig was split on a diameter and adjusted by means of wing nuts. The samples were then oven dried and thereafter cooled in either a desiccator or simply open air.

Method of Saturation

Several samples were tested in a wet, or partially saturated, condition obtained by soaking in distilled, de-aired water. It was attempted to saturate other samples by means of an aspirator. These samples were placed in plastic membranes fitted with rubber stoppers on each end and O-rings placed around each membrane to prevent flow around the rock sample. The entire jacketed sample was submerged in water and connected by means of plastic tubing to the aspirator. A central hole in the upstream

stopper allowed flow through the sample under a hydraulic gradient of one atmosphere.

Since only approximately 80 percent saturation was obtained using the above method another procedure was developed. The samples were placed in a plastic chamber and subjected to a vacuum for at least 24 hours. At the end of this time, distilled, de-aired water was injected into the chamber so that the entire chamber was filled while still under vacuum. The samples then soaked for two days before the relative success of the method was determined. Saturations of 93 to 98 percent were obtained in this manner.

Description of Membrane and Membrane Seal

A suitable material for use as a membrane must have these qualities: (1) it must be impervious with respect to the confining fluid, and (2) must be sufficiently flexible so that the sample deformation is not restricted. A material meeting these specifications is vinyl plastic in the form of thin wall tubing. The tubing used was 7/8 inch inside diameter with a 0.035 inch wall thickness. It was cut in approximately 3-1/2 inch lengths so as to slip over the steel pedestal on the base of the triaxial cell, and over the upper loading block which was placed between the piston and the rock sample. The overlapping ends of the membrane were sealed by placing 3/4 inch diameter O-rings over the jacket.

To test the membrane and its seals for leakage an oven dry limestone sample was placed in the triaxial cell and the lateral pressure increased to 10,000 psi. When the pressure was released and the sample removed, it was examined for any spots of oil which would readily be visible on the light colored surface. On only two occasions out of more

than 160 tests did the author observe any failure of the membrane. One failure resulted because a sufficient initial load on the piston (about 200 pounds) was not reached prior to applying the confining pressure. The membrane was squeezed into the small gap between the lower loading block and the pedestal. When the axial load was applied the membrane was ruptured. Another failure resulted when a granite sample was subjected to a large amount of strain after failure. As the sample moved on its rupture plane the lower end of the sample punctured the membrane. However, nearly eight percent strain had been reached prior to failure.

Thus, the vinyl membrane proved more than satisfactory for jacketing rock specimens.

Assembly and Operation of the Testing Apparatus

The technique of assembling the testing apparatus was gained primarily through experience. After the core sample, along with the loading blocks and membrane, was placed on the cell pedestal, the rubber O-rings were slipped over the ends of the membrane. At this point, in the pore pressure tests, the hose from the pressure maintaining device was connected to the cell and water pumped into the jacketed sample so as to expel any air in the system. Next, the cylinder was assembled to the base and filled with hydraulic fluid to the level of the vent valve opening. The packing gland was then secured in position, but remained at least 1/4 turn from a fully tightened condition. While the packing gland was being tightened the vent valve was opened to allow excess oil and air to escape. After assembly the triaxial cell was placed in the testing machine and the lateral confining pressure hose connected to it

from the accumulator. An initial load of 200 pounds was placed on the sample for reasons explained above, and the confining pressure applied.

An initial deformation rate of approximately 0.01 inches per minute was used in all tests. Load readings were taken at regular intervals of deformation, in some tests at 0.001 inch intervals, in others at 0.005 inch intervals. As each sample approached failure the difference between consecutive load readings became smaller. At failure the load either increased only slightly, remained constant, or decreased rapidly. The deformation rate was increased to 0.02 inches per minute after failure.

In nearly all tests the lateral pressure increased when the amount of strain exceeded the rupture strain; thus, the pressure accumulator was used to keep this pressure at a constant level. Pore pressures, on the other hand, generally showed a small decrease at failure which was likewise adjusted by the accumulator.

The high internal pressure in the cell would jam the threaded packing gland; therefore, when removing the sample, it was necessary to first tighten this part to break it loose, and then unscrew it. A large socket wrench, strap wrench and C-clamp were used in the assembly and disassembly of the triaxial cell.

Microscopic Observations

Several core samples were observed under a binocular microscope and a few cross-sections were photographed. An examination was made of unstressed samples to observe the grain structure and cementation. Also, the failure surfaces were examined to determine grain distortion, cleavage, and crystalline shear fracture.

CHAPTER VI

RESULTS

Stress - strain Curves

The stress and strain calculations for all of the samples tested were plotted compositely for each rock (Figures 19 - 22). All the curves indicate that Hooke's law, upon initial loading, is valid for rock up to a limiting stress level. On some of the curves this limiting or yield stress is clearly defined and rupture takes place almost immediately after it is reached. The Pottsville sandstone and Stone Mountain granite samples failed in this manner, thus fitting the description of brittle materials. A brittle material is defined (3) as one which will accept only a limited amount of strain after yield before rupture. The Indiana limestone and Georgia marble failed in a brittle manner under confining pressures less than 5000 psi. At greater confining pressures however, rupture occurred only after a large increase in strain. Under even higher confining pressures no well defined rupture occurred. Instead, as the stress level continued to increase, there was a continuous yield or slip. This indicates a transformation of these materials to the ductile condition when surrounded by a sufficiently high confining pressure, as observed by Serata (30). This observation is consistant with those of von Kármán, Robinson, et al.

It is important to define precisely the failure condition when determining the maximum deviator stress. In brittle failure, a peak strength is reached and the sample fractures. This peak represents a

failure condition. On the other hand, ductile failure presents no peak stress value to clearly define a maximum deviator stress. Instead, it is noted that as strain is increased well beyond initial slip, which is assumed to occur at the proportional limit, the stress - strain curve again becomes linear. Topping (35) suggested the point of intersection of the two straight protions of the stress - strain curve as a yield criterion. Another criterion, which is generally known as the offset method, uses the intersection cf the stress - strain curve and a line parallel to the initial straight portion of the stress - strain curve, which passes through some percentage of the strain, usually 0.2 percent. Topping points out that the offset method does not locate any significant transition in the stress - strain curve. The percentage of strain selected for the offset method certainly must vary according to the material tested and also the test conditions, such as confining pressure, strain rate, etc.

Topping (35) not only considers the variation of failure strain for different materials, but also the behavior of these materials in their plastic or ductile condition.

Jeffreys' failure condition (19) is similar to Topping's but has the additional significance that a strain value corresponding to a point actually on the stress - strain curve is considered. His limiting condition may be interpreted as the point where the rate of change of the stress - strain curve becomes a minimum and remains constant thereafter. This point has a mathematical significance, namely:

$$\frac{d^2\sigma}{d\varepsilon^2} = 0 \quad ,$$

which also indicates that the minimum value of the tangent modulus has been reached. (Tangent modulus is defined as the instantaneous slope of the stress - strain curve.) A comparison of these three methods is shown in Figure 4.

The Triaxial Test Results

The maximum deviator stress is, by definition, the difference between the principal stresses at failure, that is, $(\sigma_1 - \sigma_3)$. The maximum shear stress applied to the rock specimens during these tests is equal to one-half the maximum deviator stress, or:

$$\tau_{max} = 1/2(\sigma_1 - \sigma_3) \ .$$

Also, the maximum shear stress is the radius of the Mohr stress circle; the center of this circle is located at $1/2(\sigma_1 + \sigma_3)$ on the σ axis. The variation of the radius of the Mohr circle with the distance from the σ, τ origin to the center of the circle is the function:

$$1/2(\sigma_1 - \sigma_3) = F\left[1/2(\sigma_1 + \sigma_3)\right] \ .$$

The results of the triaxial shear tests are presented in this form as shown in Figures 23 - 26.

Variation of Maximum Deviator Stress with Confining Pressure

According to the maximum stress theory and maximum octahedral stress theory, the normal stress acting on the slip surface is without influence on the shear strength. The results depicted in Figure 27 contradict this view. It has been shown that the normal stress on a slip surface, along with the shear stress, is a function of the principal stresses. In the

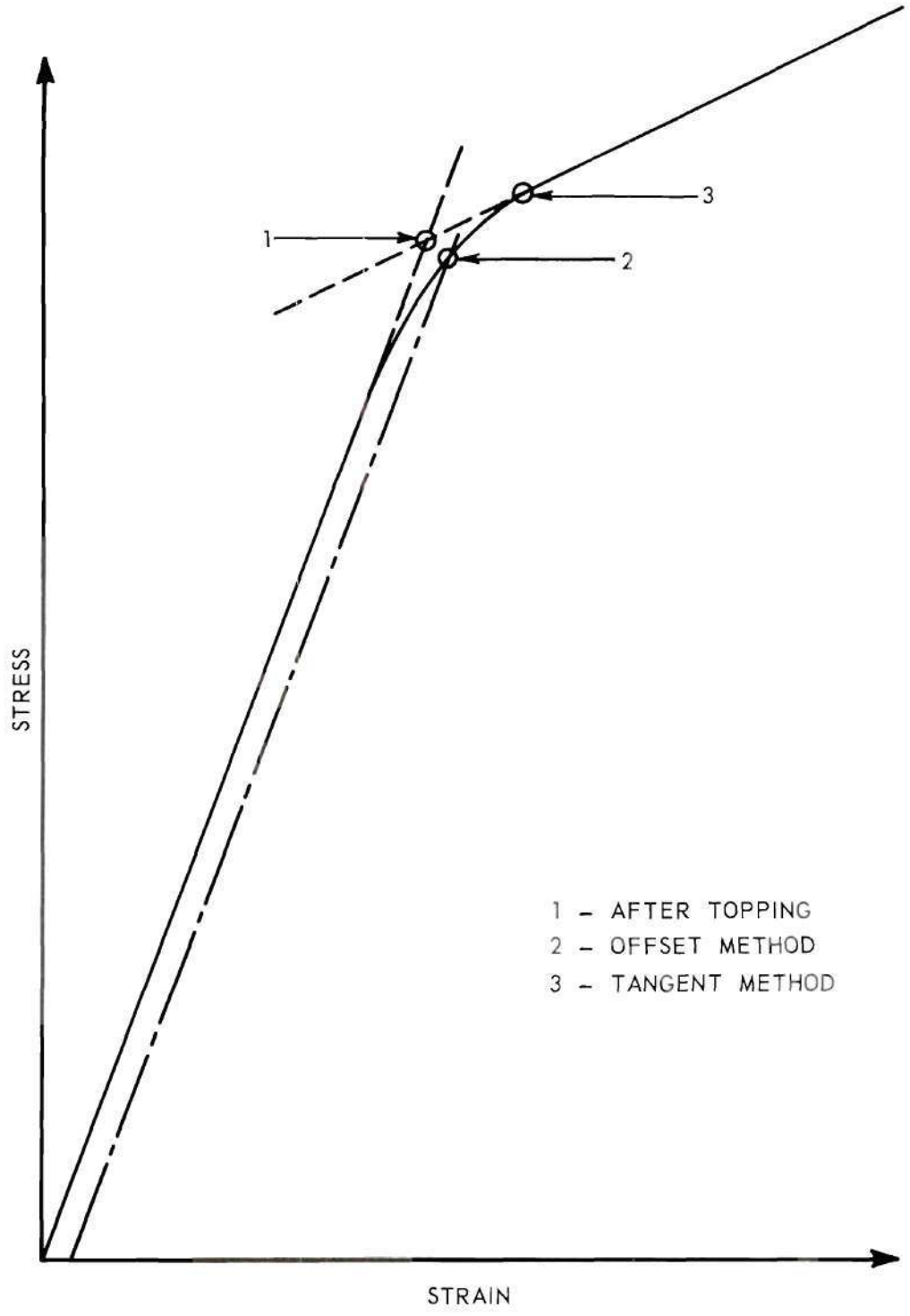

Figure 4. Criteria for Defining Maximum Deviator Stress.

present triaxial tests the confining pressure is identical with the minor principal stress. The maximum deviator stress is determined by the failure criterion.

The influence of confining pressure on strength is much greater for the granite and sandstone as compared with the limestone and marble data. In all cases, however, the strength of each rock was increased by the greatest increment under initial confining pressures. As confining pressures increased further, the corresponding increases in rock strength became less and less. At high confining pressures (above 5000 psi) the strength of the Indiana limestone was nearly constant.

Mohr's Circles of Stress and Their Envelope

The limiting stress conditions at a point are represented by the Mohr stress circle. Each set of principal stresses has a unique circle which is defined by the minor principal stress (confining pressure) and the deviator stress. For a given confining pressure the value of the deviator stress was taken from the curves shown in Figure 27 which represent the average test values. With these deviator stresses, a set of circles was drawn for each type rock (Figures 28 - 31).

According to Mohr, the envelope of these circles is the critical stress function,

$$\tau = f(\sigma).$$

This envelope has a true physical significance because it represents a limiting curve of the possible stress combinations in a given material. The Coulomb-Mohr theory approximates this envelope by a straight line represented by the equation:

$$\tau = \tau_o + \sigma_N \tan \varphi \quad .$$

It is clear that the envelopes illustrated can not be described completely by such an equation. Two distinct portions of each envelope are observed, one portion being non-linear, the other linear. If each envelope is projected along its straight line segment a pseudo-intercept may be found on the shear stress axis. Of more interest is the actual intercept of the non-linear portion of the envelope which is shown on a larger scale in Figure 32. To better define the shape of the envelope in this region, tension tests were conducted which give a "negative" stress circle. It was then assumed that the tensile strength developed in the material under a condition of pure shear would be the same as that in simple tension. A circle representing a condition of pure shear is shown drawn about the origin of the σ, τ axis (Figure 32). It is noted that the shear circle drawn in this manner represents the only possibility for both it and the simple tension circle to be tangent to the envelope. The tensile strength and shear intercept for each rock is given in Table 2.

Linearity and Non-linearity of the Rupture Envelope

As previously mentioned, a portion of the Mohr envelope for each rock is a straight line. In order to evaluate the non-linear portion of the envelope, a line parallel to the straight line portion of the envelope was drawn through the shear axis intercept of the envelopes shown in Figures 28 - 31. The vertical distance from this line to the envelope was measured for various values of normal stress. This measurement, termed fracture interference, by the present author, is shown as a function of normal stress in Figure 6.

Table 2. Tensile Strength and Shear Axis Intercept

Type Rock	Tensile Strength (psi)	Shear Axis Intercept (psi)
Indiana Limestone	392	1100
	375	
	317	
Pottsville Sandstone	437	1300
	441	
Stone Mountain Granite	500	1800
	940	
	1092	
Georgia Marble	650	1000
	650	

For a further comparison of the fracture interference in each rock, the ordinates of the curve shown in Figure 6 were divided by the shear intercept, τ_o, and cos φ_{min}. These ratios were also plotted as a function of normal stress as shown in Figure 7. The remarkable uniformity of the "parameter ratio" regardless of the type of rock suggests a general expression for the non-linear portion of the rupture envelope. It is illustrated further that this ratio becomes constant at normal stress values between 10,000 and 15,000 psi.

Angle of Failure Planes

The condition of the core samples after testing can be clearly seen in Figures 10 - 14. A single distinct failure plane was observed for each sample which exhibited brittle fracture. However, numerous slip planes and bulges were observed when the samples failed in a ductile manner. The angle between the failure plane and the axis of the core sample was measured whenever a slip surface could be clearly distinguished. These planes were so numerous in some of the limestone and most of the marble samples that the core surfaces appeared mottled.

A predicted angle of failure was determined from the Mohr stress circles (see Appendix) and the rupture envelopes. A comparison of predicted angle and measured angle is given in Table 3.

Failure planes for the tensile tests are exhibited in Figure 14. These planes appear to be nearly perpendicular to the core axis. This angle corresponds exactly to that predicted by the Mohr envelope.

Pore Pressure Tests

The results of the pore pressure tests are shown in Figures 33 - 36. Each test was conducted under an external confining pressure of 5000 psi.

Table 3. Comparison of Measured and Predicted Angle of Slip (degrees)*

Type rock	Indiana Limestone		Pottsville Sandstone		Georgia Marble		Stone Mountain Granite	
Lateral pressure (psi)	Observed angle	Mohr's angle	Observed angle	Mohr's angle	Observed angle	Mohr's angle	Observed angle	Mohr's angle
0	15	24	16.5	18	obscured	20.5	10	17.5
1000	25	31	15	19	"	25	18.5	17.5
2000	30	35	20	21	"	29.5	19	19.5
3000	37	38	25	26	"	32	20	20
4000	42	39	26	26	"	33	-	21
5000	45	41.5	26	26	"	33.5	23.5	23
6000	45	44	25	26	"	34	20	24.5
7000	45	45	28	26	"	36	27	24.5
8000	45	45	27.5	26	"	36	28	24.5
9000	obscured	45	26.5	26	"	36	25	24.5
10000	"	45	28	26	"	36	18	24.5

*Slip angle was measured between direction of slip plane and the vertical axis of the sample.

The interstitial pressure was held constant throughout the test by means of the accumulator. Deviator stresses were measured for samples subjected to pore pressures of 1000, 3000, and 5000 psi. The maximum deviator stress obtained was compared to the average strength of dry samples which were confined by a pressure equal to the difference between the pore and confining pressures applied to the saturated samples.

The void ratios of the limestone and sandstone samples were approximately 0.20, whereas the granite and marble specimens had values of approximately 0.020. The first two rocks are, therefore, classified as porous; the latter two are nearly impervious. The strength of the porous rocks was essentially the same whether tested dry or saturated when compared using the concept of "effective confining pressure." On the other hand, the strength of the impervious rocks has no correlation with the "effective confining pressure." The maximum deviator stress obtained for the granite and marble cores was nearly the same for all values of applied pore pressure.

A series of tests was conducted to determine the "softening" effect of water for the limestone and sandstone. Test specimens of these rocks were prepared by soaking them in water at room temperature under atmospheric pressure. The samples reached varying degrees of saturation ranging between 60 and 80 percent. These were placed in the triaxial cell and tested with the pore pressure inlet valve open to the atmosphere so that any pore pressure increase would be dissipated. The Pottsville sandstone samples had wet and dry strengths nearly equal. The Indiana limestone strength values fell in the same scatter range for both wet and dry specimens, but the average strength of the wet samples was slightly lower than the average strength of the dry samples.

Microscopic Study

Each sample was examined under a binocular microscope to determine the grain structure prior to testing and its condition on the failure plane after fracture. The former has been mentioned in the description of the rock samples.

The shear planes of the limestone samples appeared slickensided which gives evidence of granulation and fracture of particles in the shear zone. These fractured particles were dull and had a gel-like appearance. A powder was observed on the slip surface indicating granulation of particles in the shear zone.

The shear plane of the sandstone appeared rough and irregular. The crystals on this surface were either broken or pulled apart, forming a powder of variable particle size. After the powder had been removed, the surface appeared much the same as the cross-section prior to testing.

The Stone Mountain granite consists of a wide variety of minerals which showed many cleavage planes in the slip surface. A powder similar in all respects to that found on the sandstone was observed.

The Georgia marble, as previously mentioned, consists of nearly pure calcite crystals. Numerous slip surfaces were developed by the triaxial compression so that the core samples disintegrated when removed from their vinyl jacket. The crystals examined under the microscope were highly broken and of variable particle size. In addition, perfect cleavage of many crystals could be clearly observed.

CHAPTER VII

DISCUSSION OF RESULTS

Summary of Conclusions

The objectives of this investigation have been: (1) selection of a criterion to determine the failure condition for rock, (2) evaluation of the factors contributing to the shear strength of rock, (3) a mathematical representation of shear strength parameters, and (4) examination of the effect of interstitial fluid pressure.

Based on a critical review of literature in the field of rock mechanics and experimental studies by the author, the following conclusions have been reached:

(1) The tangent method proposed by Jeffreys is most suitable for the determination of maximum deviator stress.

(2) Rock fails by either splitting, shear, or a combination of these - pseudo-shear.

(3) Failure of rock is ductile or brittle depending upon the amount of confinement.

(4) Shear failure will occur in rock if confining pressures are sufficient to prevent splitting.

(5) The angle of slip for shear failure is closely predicted by the Mohr criterion.

(6) Shear strength of rock may be considered the sum of cohesion, internal friction, and "fracture interference."

(7) Fracture interference appears to be a unique function of normal stress for all the rocks tested.

(8) The concept of "effective confining pressure" is not universally valid.

Discussion

The maximum deviator stress when the failure condition is reached in a brittle material is clearly defined by the stress - strain curve for the material. These curves (Figures 20, 22) for the Pottsville sandstone and Stone Mountain granite illustrate that these rocks failed by brittle fracture for all confining pressures. Therefore, the maximum deviator stress is defined as the peak value of the stress - strain curve.

The Indiana limestone and Georgia marble (Figures 19, 21) failed in the same manner under confining pressures up to 5000 psi. Beyond this confining pressure both rocks supported additional load as strain increments were increased well beyond the point of initial yield. Initial yield is defined as the stress condition beyond which stress and strain are no longer proportional. These latter stress - strain curves thus have no maximum value but do reach a point where stress and strain again become linear. Von Kármán, 1911 (20), observed similar data for Carrara marble and commented that a failure stress could not be determined for stress - strain curves which continued to slope upward.

Various investigators, however, have utilized one method or another to resolve this difficulty caused by ductile failure. In many cases the offset method has been used to predict a yield stress. However, this method cannot account for the final stress - strain behavior of a ductile material, since the selection of failure stress reflects only the initial

slope of the curve, and an arbitrarily chosen percentage of strain. Therefore, physical reality cannot be satisfied by the offset method. Topping, 1955 (35), has suggested another criterion (see p. 37) which takes into consideration the plastic behavior of the material. The present author has used the point on the stress - strain curve where $d^2\sigma/d\varepsilon^2 = 0$ to define the maximum deviator stress. This is an extension of Jeffreys' failure criterion which is discussed on p. 38.

The modes of rock failure which have been observed in this investigation are: tension or splitting, shear, and a combination of these called pseudo-shear. These modes are illustrated in Figures 10 - 13. Terzaghi, 1945 (34), described each of these failure modes which had also been observed by Griggs, 1936 (13), and von Kármán, 1911 (20). Griggs attributes the tension or splitting failure to the wedging action of shear planes which causes a failure of the bond between grains. Terzaghi proposes that intermediate grains force their way between two adjacent grains causing them to separate. In either case a crack is initiated which gives rise to highly concentrated stresses at the crack vertex. Griffith, 1921 (12), proposed that these cracks could account for failure in all materials. (See Appendix for discussion of Griffith's theory.)

A clear distinction has been observed between tension and shear failure surfaces in the present study. Griggs, 1936 (13), noted this difference even though his samples were tested in the absence of a membrane to separate the confining fluid from the rock. The current author has observed these failure surfaces under a binocular microscope and studied microphotographs, typical of which appear in Figures 15 - 18. The tension surfaces appear as a fresh break in the rock showing a clear separation

of particles. Shear failure, on the other hand, produces a surface which is covered by granulated particles of variable size. Several specimens also failed by a combination of shear and tension.

The transition from brittle to ductile failure as confining pressures were increased from 0 to 10,000 psi was observed for the limestone and marble. No ductile failure was produced for the granite and sandstone by the triaxial apparatus used in the present investigation. However, the high pressure studies reported by Bridgman, 1952 (10), have indicated that all materials may eventually become ductile if tested under sufficiently high confining pressures.

Another significant transition which occurred in all the rocks tested was the progression from tension failure to pseudo-shear, and finally, shear failure which accompanied corresponding increases in confining pressure. In other words, the tension produced between grains is gradually reduced by the superposition of hydrostatic pressure until eventually, the sum of the forces between grains is totally compressive. Tensile cracks are thereby prevented in the same manner prestressing prevents tensile failure in structural concrete. If splitting is completely prevented, the samples fail by shear and produce the slip planes shown in Figures 10 - 13. Failure by pseudo-shear occurs, therefore, when splitting is only partially prevented.

Terzaghi's observation (see p. 15) that, as pure shear failure is approached, the slope angle of the failure surface can be successfully predicted by the Mohr envelope is confirmed by the comparisons made in Table 3. In his failure criterion, Mohr presumes that fracture occurs as a result of a critical combination of shear and normal stress on the slip

plane (see Appendix). The effect of the intermediate principal stress is, therefore, neglected. Also neglected is the local tensile force between points of contact of individual grains which has been shown to become of more importance as confining pressures are reduced. If tensile failure alone causes fracture, the failure plane is parallel to the direction of the deviator stress which, of course, is not predicted by the Mohr criterion. A combination of tension and shear produces a "zig-zag" failure surface which is shown most clearly by the granite specimens under confinements from 0 to 3000 psi (Figure 13). Therefore, only when this tensile failure is prevented can the failure angle be accurately predicted by Mohr's theory.

Shear strength of cohesive materials as viewed by Hvorslev (18) and later discussed by Lambe (21) is influenced by three properties of the material: (1) cohesion, (2) internal friction, (3) dilatancy. The term dilatancy actually refers to a volume change which is a result of one particle blocking the path of another as slip is initiated on a glide plane. A preferred terminology for this phenomenon would be particle interference. Therefore, the term "dilatancy" has been replaced throughout the present report by its more descriptive synonym.

Cohesion is defined as the inherent shear strength of a material in the absence of external stresses. Physically, it is the resistance to particle separation without the influence of any external forces or pressures. This resistance to separation consists of molecular bonding, ionic attraction, van der Waals forces, and particle interlocking. A laboratory procedure for direct evaluation of cohesion has not yet been developed. However, an estimate of cohesion is obtained by considering

material strengths under the influence of both positive and negative normal stresses and plotting Mohr's circles for these stresses. These strength values are obtained by conducting tension and compression tests. An interpolation between these values to obtain the shear strength at zero normal stress, by means of the Mohr envelope, is the approximate cohesive resistance of the material. This procedure is illustrated in Figure 32.

Internal friction and particle interference cannot in reality be evaluated separately since these properties are dependent on each other. Borowicka (7) postulates that crystalline solids, which show a frictional component of shear strength, must have interior surfaces. He regards each crystal as an independent cell or element; thus, the frictional strength of the entire aggregate of crystals is developed when one crystal face is pushed against an adjacent crystal face.

Microscopic studies conducted by the present investigator have shown (Figures 15 - 18) that particles in the slip zone of the samples failing by shear are granulated. Therefore, internal friction and particle interference not only involve a mutual slipping of adjacent particles but also fracturing and cleavage of individual grains. That part of particle interference which is due to fracturing of grains is called "fracture interference" by the present author.

It is proposed that the slope angle of the final linear portion of the Mohr envelope be interpreted as the friction angle of the granulated material in the shear zone. The angles thus measured from the envelopes in Figures 28 - 31 are values which could be reasonably expected for soils having similar gradation, particle size, and density as the crushed rock in the failure zone. These angles are 38.6 degrees for the Pottsville

sandstone and 42 degrees for the Stone Mountain granite which are both typical of fine grained, dense, cohesionless soils. An angle of 20 degrees was measured for the Georgia marble which can be compared to the friction angle of calcite crystals. The final slope of the envelope for the Indiana limestone was horizontal. The material in the shear zone of the limestone was completely fractured which indicates that the shear resistance was due to the breaking of individual crystals rather than a frictional resistance of one crystal sliding over another. This shear resistance is, then, independent of external pressures and the angle of internal friction for this condition would logically be zero.

The test results are presented in terms of stress circles and a rupture envelope (Figures 28 - 31). Each envelope is represented by:

$$\tau = f(\sigma_N) \quad .$$

In order to express this curve in terms of shear strength parameters, cohesion, internal friction (which includes some particle interference), and fracture interference are considered separately. A typical Mohr envelope is shown in Figure 5. The shear strength of rock is expressed in general as:

$$\tau_{ult} = \tau_o + \bar{\sigma}_N \tan \varphi_{min} + I_p \quad ,$$

where τ_{ult} = failure shear stress,

τ_o = cohesion (shear intercept at zero normal stress).

$\bar{\sigma}_N$ = effective normal stress,

φ_{min} = minimum slope angle of the Mohr envelope,

I_p = fracture interference function

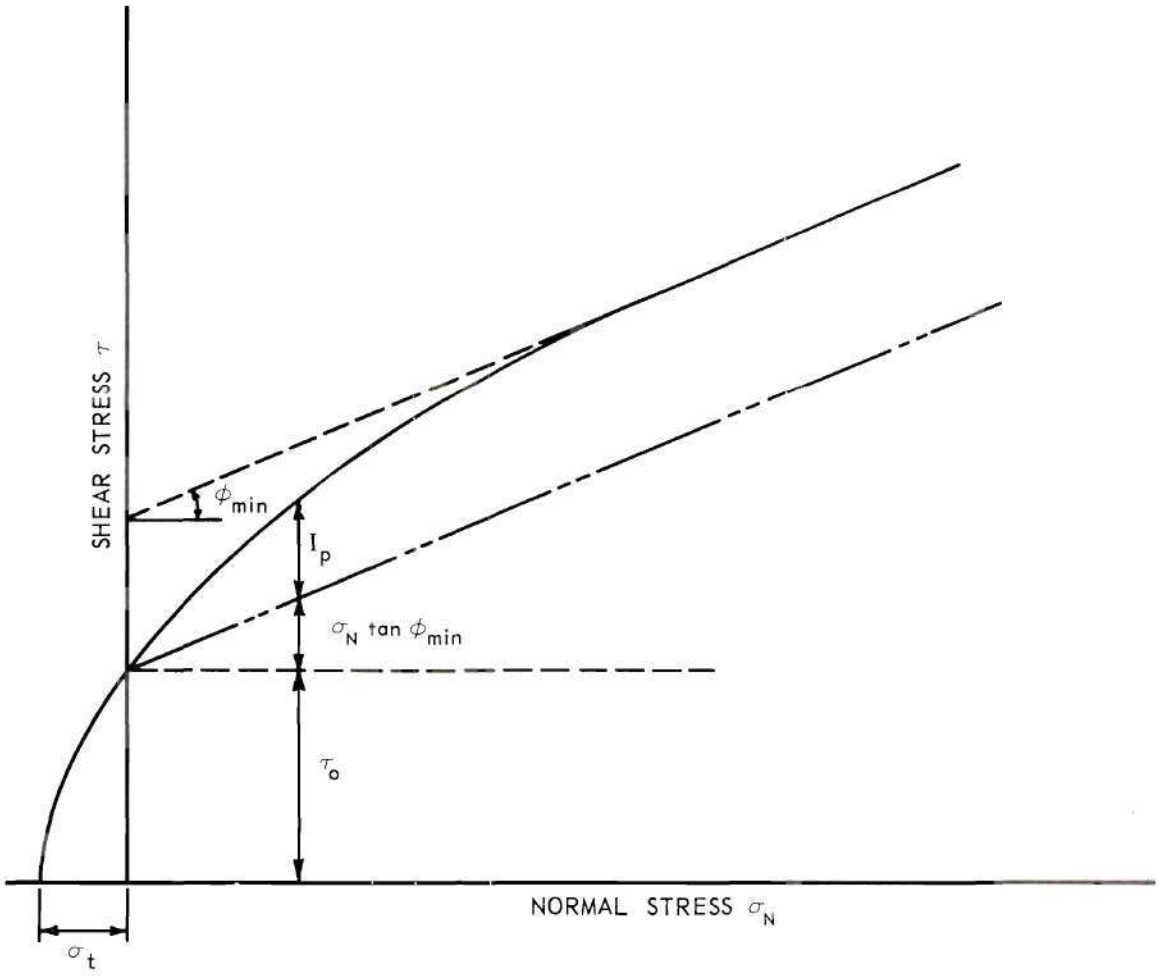

Figure 5. Typical Mohr Envelope.

The fracture interference parameter as a function of normal stress is examined for each rock (Figure 6). Although these rocks have a wide variety of strengths as seen in Figure 27, the range of values for a given normal stress is very small in comparison to the strength differences. Also of interest is the fact that these parameters eventually approach a unique constant. This constant parameter value is interpreted in the following manner. As confining pressures are increased and splitting failure is essentially prevented, the number of grains fractured in the shear zones per unit length becomes constant. The failure shear stress, therefore, becomes a linear function of normal stress.

The "fracture interference" parameter, I_p, represents the curvilinear portion of the Mohr envelope between zero normal stress and the point where shear strength becomes a linear function of normal stress. This transition depends upon the material properties at each end of the curvilinear section of the Mohr envelope. These properties are the shear intercept, τ_o, and the "shear failure angle of friction," φ_{min}. In order to compare the "fracture interference" parameter for each rock tested, it is necessary to "normalize" the parameter, I_p, with respect to the material properties, τ_o and φ_{min}. Thus, a "parameter ratio" has been evaluated for each rock tested:

$$\text{parameter ratio} = \frac{I_p}{\tau_o \cos \varphi_{min}} \quad .$$

The functional relationship between "parameter ratio" and normal stress is shown in Figure 7. The test results suggest that this ratio represents a unique relationship for all rocks.

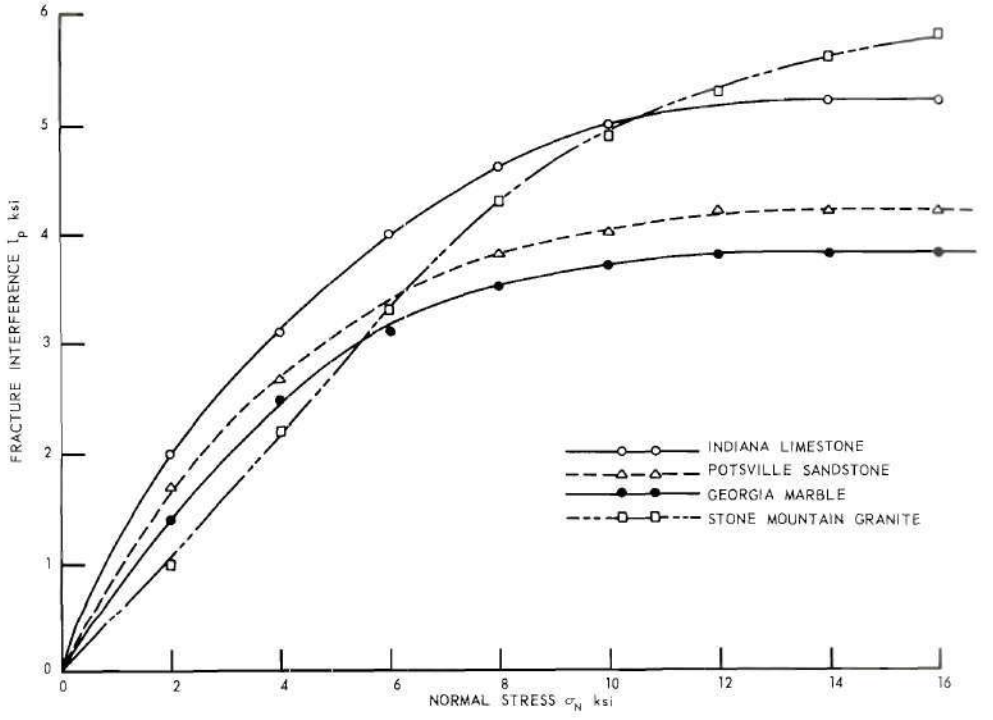

Figure 6. Fracture Interference vs. Normal Stress.

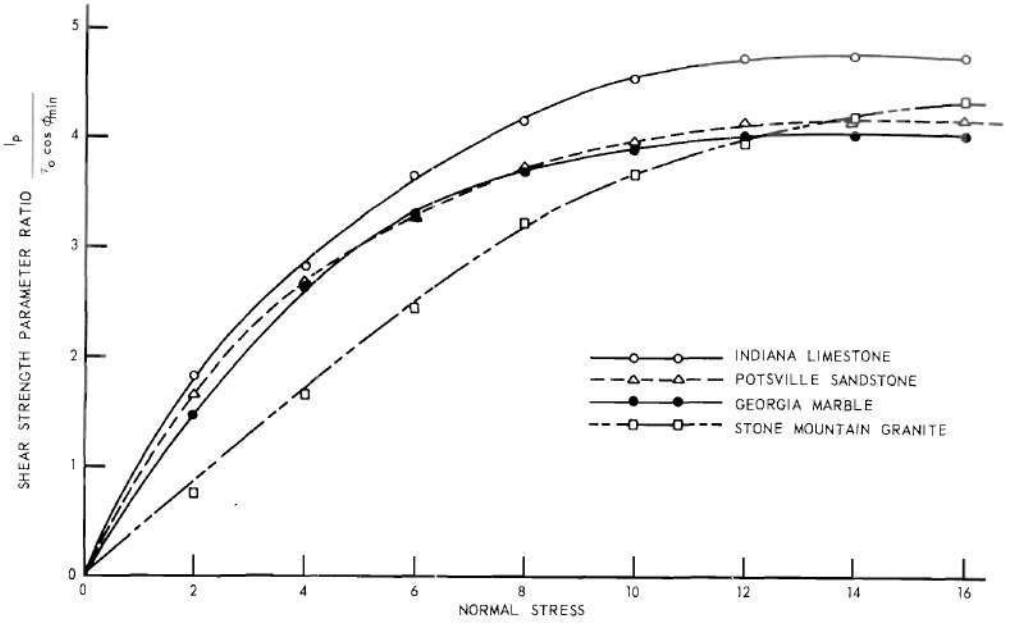

Figure 7. Parameter Ratio vs. Normal Stress.

The effect of interstitial pressure has been examined using distilled, deaired water to saturate the rock specimens. During each test the pore pressure was held constant while strain was applied at the same rate as used for the dry tests. Robinson (27) and Serdengecti and Boozer (31) have examined the strength of porous rocks under the influence of interstitial pressures. They have concluded that Terzaghi's equation for effective stress may be used for all rocks. The results of the tests (Figures 33 - 34) on limestone and sandstone concur with the finding of Robinson and Serdengecti. The present investigation has shown that this conclusion is only valid for rocks of relative high porosity in which the pore spaces are probably continuous. On the other hand, Terzaghi's equation can not be used to account for the behavior of the nearly impervious granite and marble. Skempton (38) has presented an equation derived from theoretical reasoning which may more correctly express the effective stress in fully saturated concrete and rock.

The strength of the saturated granite and marble was, however, significantly reduced as shown in Figures 35 - 36. This reduction in strength appears to be the same regardless of the applied pore pressures. It is concluded, therefore, that the pore cavities in these samples are not continuous or completely interconnected and the concept of effective confining pressure is not universally valid. Also, the lower strength values of the rocks may be the result of a softening of the bonds between the constituent minerals in the presence of water. Since all samples were initially wet, due to the coolant during coring, their strength is regained when they are throughly dried.

CHAPTER VIII

RECOMMENDATIONS FOR FURTHER STUDY

The foregoing investigation has left many problems unsolved and presented new ones. It is recommended that the following be studied:

(1) determination of the continuity of pore spaces in dense rock,

(2) investigation of the pore pressure build up and dissipation using long duration tests,

(3) improved methods of saturation for rocks of low permeability,

(4) investigation of crystalline lattice deformation during mineral shear failure,

(5) determination of the parameters of molecular attraction and repulsion in mineral crystals,

(6) examination of the non-linear portion of the rupture envelopes of several other rocks,

(7) evaluation of the effect of the intermediate principal stress on rock failure, and

(8) evaluation of isotropic and anisotropic strength properties for various rocks.

APPENDIX

The first section contains fundamental theories which are used to describe stress conditions, physical properties, and failure of polycrystalline materials. In the second section are the data and illustrations of the present research.

STRESSES

Mohr's Representation of Stress at a Point (23)

Consider the equilibrium of a cubical element subjected to co-planar stresses. Each face of the element is subjected to a shear stress and a normal stress. Under plane stress this element may be so rotated that the shear stresses vanish and the corresponding normal stresses reach a maximum and minimum value. These normal stresses are known as principal stresses. If we now consider an oblique plane through an element subjected only to principal stresses we may write the equilibrium equations and solve for the shear stress and normal stress on this oblique surface:

$$\sigma = \frac{\sigma_1 + \sigma_3}{2} + \frac{\sigma_1 - \sigma_3}{2} \cos 2\alpha \ ,$$

$$\tau = - \frac{\sigma_1 - \sigma_3}{2} \sin 2\alpha \ .$$

If we arrange these equations so as to eliminate the trignometric functions we have:

$$[\sigma - 1/2(\sigma_1 + \sigma_3)]^2 + \tau^2 = [1/2(\sigma_1 - \sigma_3)]^2 (\cos^2 \alpha + \sin^2 \alpha)$$

or

$$[\sigma - 1/2(\sigma_1 + \sigma_3)]^2 + \tau^2 = 1/4(\sigma_1 - \sigma_3)^2 = \text{constant.}$$

Thus, if we construct a coordinate system having a σ and τ axis, the above equation describes the circle shown in Figure 8. Each point on the circle represents a unique combination of shear stress and normal stress; the total circle, then, represents all possible such combinations. A radius of the stress circle represents the direction of normal stress. Angles measured between radii are twice the physical angle between normal stress directions.

Octahedral Stresses (25)

The maximum and minimum values of shear stress may be found considering the equation:

$$\tau = \pm 1/2(\sigma_1 - \sigma_3) \sin 2\alpha$$

such that:

$$\tau = \pm 1/2(\sigma_1 - \sigma_3)$$

for the values of $\alpha = 45°$ and $\alpha = 135°$ respectively.

There are three principal stress circles for the general state of stress at a point whose centers are $1/2(\sigma_1 + \sigma_2)$, $1/2(\sigma_2 + \sigma_3)$, and $1/2(\sigma_1 + \sigma_3)$ on the σ axis. The radii of these circles represent the "principal shearing stresses":

$$\tau_1 = 1/2(\sigma_1 - \sigma_2) \quad ,$$

$$\tau_2 = 1/2(\sigma_2 - \sigma_3) \quad ,$$

$$\tau_3 = 1/2(\sigma_1 - \sigma_3) \quad ,$$

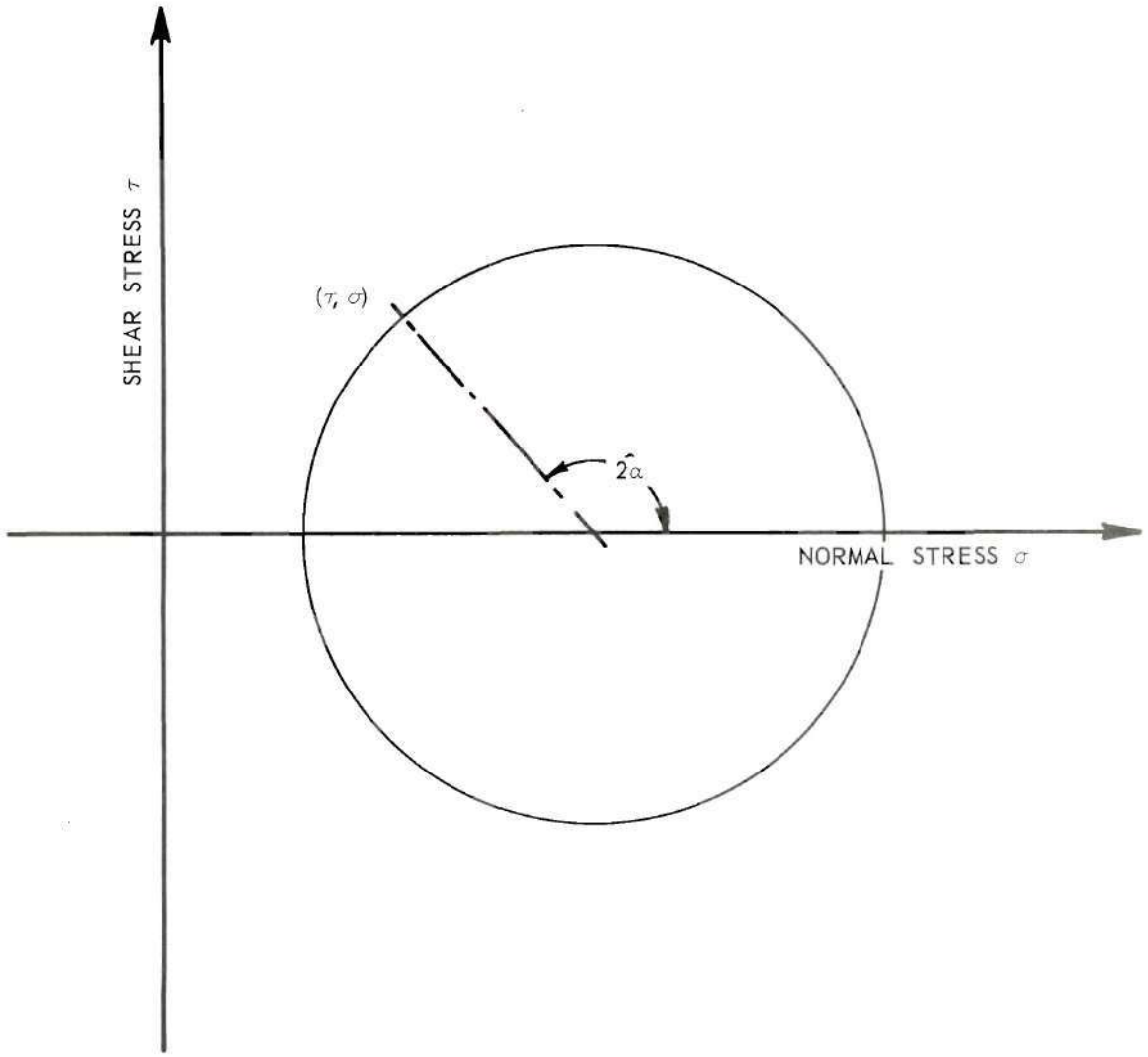

Figure 8. Mohr's Circle of Stress.

such that

$$\tau_1 + \tau_2 + \tau_3 = 0 \quad .$$

The direction of the principal shearing stresses form a regular octahedron whose corners lie upon the principal axes. If we choose an oblique plane having direction angles $\alpha = \beta = \gamma = \cos^{-1}(1/\sqrt{3})$ (this plane is one face of the octahedron referred to above), the value of the normal stress (octahedral normal stress) on this plane becomes

$$\sigma_{oct} = \frac{\sigma_1 + \sigma_2 + \sigma_3}{3}$$

which is the average value of the three principal stresses. The octahedral shearing stress is given by

$$\tau_{oct} = 1/3\sqrt{(\sigma_1 - \sigma_2)^2 + (\sigma_2 - \sigma_3)^2 + (\sigma_3 - \sigma_1)^2}$$

or

$$\tau_{oct} = 2/3\sqrt{\tau_1^2 + \tau_2^2 + \tau_3^2} \quad .$$

ATOMIC BONDS

Forces Between Atoms (3)

The first consideration in discussing atomic bonds is the forces between atoms. If two atoms are initially infinitely apart their potential energy with respect to each other is zero. Upon approaching each other, they either attract or repel one another; thus, their potential energy increases to a level inversely proportional to some power of the separation distance. Considering attraction a negative potential energy and repulsion a positive potential energy, the total may be expressed by:

$$V = -\frac{\alpha}{r^n} + \frac{\beta}{r^m} \quad ,$$

where V = potential energy,

α = proportionality constant for attraction,

β = proportionality constant for repulsion.

The forces between the two atoms may be expressed:

$$F = -\frac{dv}{dr} = -\frac{n\alpha}{r^{n+1}} + \frac{m\beta}{r^{m+1}} \quad .$$

At some separation, r_e, called the equilibrium separation, the forces of attraction and repulsion are equal and the potential energy is at an absolute minimum. A great deal of work must be done to move the atoms any closer together because of the rapid increase in repulsive force as shown in Figure 9.

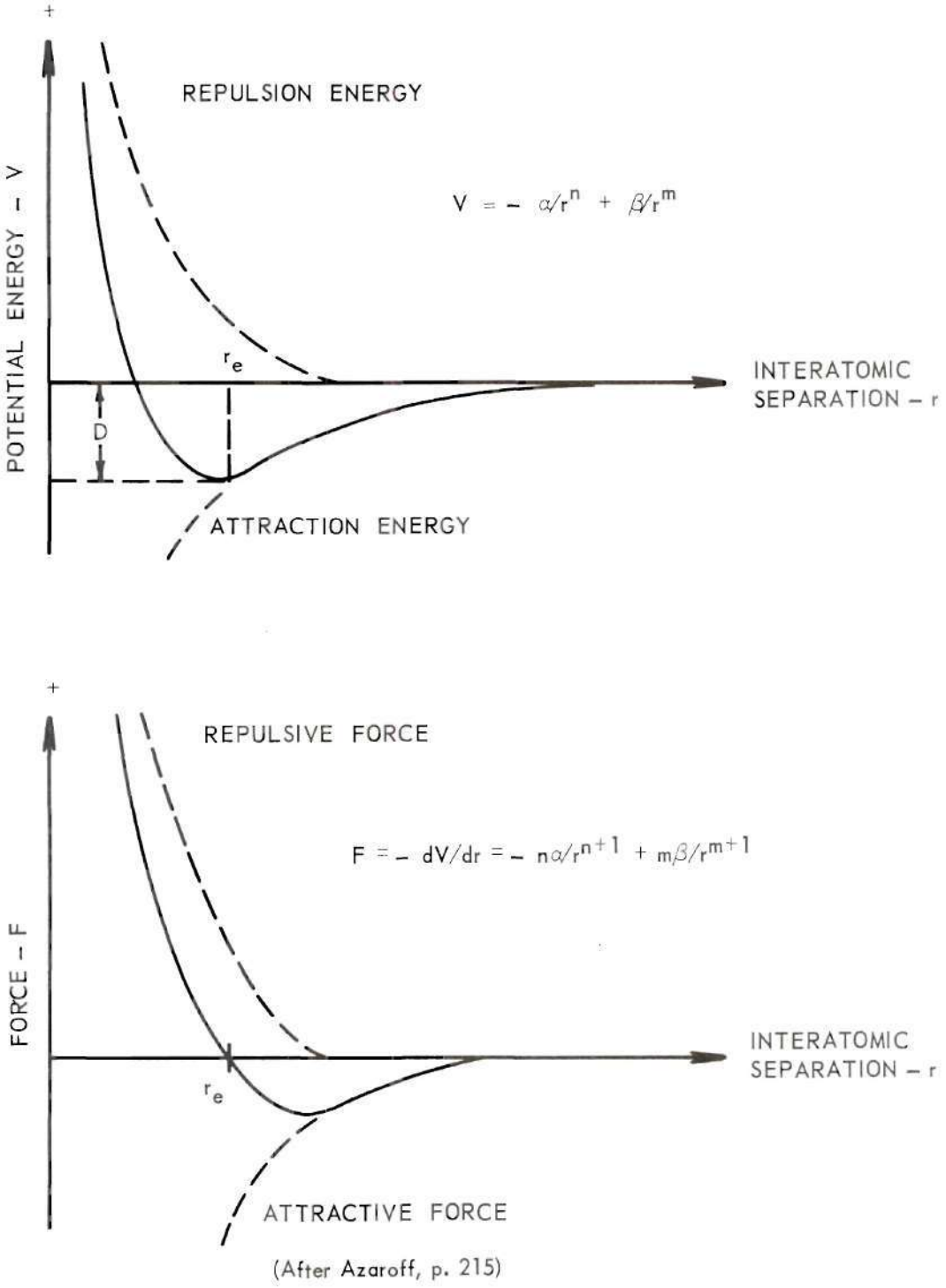

Figure 9. Energy and Force Between Atoms.

Because of nonuniformities in the electrostatic charge distribution, opposite ends of certain molecules may appear charged producing dipoles. The attraction between dipoles, either permanent or instantaneous, leads to the van der waals force which is usually small but of finite value for most solids.

When two atoms possess electrostatic charges of opposite sign, because of electron deficiency or excess, the force of attraction between them is called ionic bond. This bond is due entirely to the Coulomb attraction of two spherically distributed charges of opposite sign. Each ion tends to surround itself with as many ions of opposite sign as possible forming a continuous network. Thus, ionic crystals, rather than discrete small molecules, are produced.

The cohesion of ionic crystals is very closely approximated by considering the electrostatic energy between point charges. The potential energy may be expressed as:

$$V = -\frac{Ae^2}{r} + \frac{B}{r^n}$$

where "e" is the charge on the crystal in electron volts. Considering that at the separation distance r_e, the potential energy must be a minimum we have:

$$\left[\frac{dv}{dr}\right]_{r=r_e} = - = \frac{Ae^2}{r_e^2} - \frac{nB}{r_e^{n+1}}$$

or

$$B = \frac{Ae^2}{r_e^2} \cdot \frac{r_e^{n+1}}{n} = A\frac{e^2 r_e^{n-1}}{n}$$

The constant A, called the Madelung constant, depends on the exact crystal structure and can be evaluated for most simple structures. If the compressibility, K, of the crystal is found experimentally, then

$$K = \frac{18 r_e^4}{Ae^2(n-1)} \quad ,$$

and we may solve for the exponent, n.

Taking all energy considerations into account we may write:

$$V = \frac{Ae^2}{r} + Be^{-r/n} - \frac{C}{r^6} + \delta$$

where the third term is the contribution due to van der Waals forces and δ is a small contribution expressing the energy of the structure at zero degrees absolute temperature.

Other Bonding (3)

In addition to ionic bonding, atoms are held together by covalent bonds and, lastly, metallic bonds. Covalent bonds involve the actual sharing of electrons in the outer shells of the adjoining atoms. The number of such bonds an atom may form depends on the number of unpaired electrons in its outer shell. Metallic bonds, on the other hand, are distinguished by the so-called free electrons which are shared by all

the atoms. The free-electron theory explains the properties of high thermal and electrical conductivity, ductility, metallic luster, etc. which metals possess.

PROPERTIES OF POLYCRYSTALLINE MATERIALS

Deformation and Fracture of Polycrystalline Materials (3)

Deformation due to applied stress is classified as elastic or plastic depending on the strain recovery after the load is removed. The type of deformation in a single crystal depends only on the magnitude of the applied stress and the nature of the molecular bonds in the crystal. A polycrystalline material, however, is complicated by the random orientation of the individual crystals which causes deformation of the aggregate to differ considerably from that of a single crystal.

Of particular interest is the plastic deformation of single crystals and the corresponding aggregate solids. The actual stress required to produce plastic deformation in a crystal is several times less than the theoretical value based on the strength of the interatomic bonding. This can be explained by postulating that the intercrystalline boundaries tend to weaken the crystals so that they deform at a lower stress level. Plastic deformation involves a relative displacement of atoms along a slip plane producing slip striae, which can be observed under a microscope. Slip occurs on a potential slip surface whenever the shear stress parallel to the surface reaches a critical value. For metal crystals, Azaroff (3) points out that this shear stress is the only stress component which causes slip. The normal stress component has no effect as demonstrated by hydrostatically loading different metallic crystals.

Slip Dislocations (3)

When a sufficiently large shear force is applied to a crystal the result is a translation or a crystal twinning. This deformation however does not occur as a simultaneous displacement of all atoms in the slip plane; rather, a progressive movement takes place where, at a given time, some of the atoms are displaced while others are not. The separation between disturbed and undisturbed atoms is called a "slip dislocation" and is accompanied by dislocation lines which must either form a closed loop around the dislocation or terminate in one or two sides of the crystal. In order for deformation to continue, new dislocations must be produced in regions of stress concentration. These regions of stress concentrations are produced around inclusions or intracrystalline boundaries. A dislocation formed by an inclusion is driven by its own applied stress in the slip plane forming an ever increasing loop. As strain is continued, the dislocation loops grow externally and form new loops in a continuous process (3), p. 135. A unit dislocation has a low energy when it is parallel to the direction of slip. Unit dislocations not parallel to the slip plane may dissociate into two half dislocations which are in the directions of slip. As dislocations move under applied stress they produce jogs, thus interfering with each other. The motion of dislocations is also impeded by the presence of impurities in the substance or interstitial impurities since dislocations require additional energy to move around these obstructions. It is also possible for dislocations to move under shear stresses below the critical value since the dislocations may derive additional energy from phonons present in the crystal. This, therefore, is an explanation of creep phenomena.

Failure of crystals may be classified into two groups: (1) cleavage, and (2) shear fracture. Cleavage of a single crystal produces well defined, plane faces. Since crystals tend to cleave along certain planes only, the critical stress necessary to produce cleavage depends on the relative orientation of these planes to the direction of the applied stress. Shear fracture differs from cleavage since it leaves a nonplanar surface. Each type of failure can occur in polycrystalline materials and each distinguished for the other by the appearance of the slip surface.

Fracture is classified as brittle or ductile depending on the amount of plastic deformation before failure. Brittle fracture occurs almost immediately after the limit of the elastic properties has been reached where as ductile failure may require a strain of many times that required to reach the elastic limit before fracturing.

Crystal Twinning (3)

The formation of twins may also be considered a crystalline failure. Two crystals may be so deformed as to form mirror images of each other. Some other relationship may also exist between twinned crystals. A critical stress value for twinning exists just as a critical stress value for slip in a crystal. Twinning, however, depends on the relative orientation of the stresses within the slip and twin planes to the slip direction in addition to the orientation of the stresses relative to these planes.

FAILURE THEORIES

Comparison of Failure Criteria (32)

Failure as mentioned by Silverman (32) may be defined in several ways, such as, the initiation of yield in a material, the appearance of slip lines on external surfaces of the material, or actual rupture. It is well to relate failure conditions to the general state of stress which may be sufficiently described by stating the three principal stresses and their respective directions.

Silverman also points out that failure conditions are related to significant quantities or numbers which have dimension of either stress, strain, or energy. These three dimensions, therefore, catagorize the three basic types of failure theories. Every failure theory may be expressed mathematically by considering the failure or limiting condition as a function of the three principal stresses and a significant number based on the unconfined compressive strength.

Six failure theories are presented by Silverman along with their significant numbers and limiting conditions. These failure theories are:

1.) maximum stress,

2.) maximum strain,

3.) maximum shear,

4.) maximum octahedral shear,

5.) maximum strain energy,

6.) maximum distortion energy.

The maximum stress theory predicts failure when one of the principal stresses reaches a limiting value such as:

$$\sigma_1 = \pm \sigma_o$$

or, in general, the limiting conditions in terms of all principal stresses is

$$(\sigma_1^2 - \sigma_o^2) \cdot (\sigma_2^2 - \sigma_o^2) \cdot (\sigma_3^2 - \sigma_o^2) = 0 \quad .$$

This theory, however, fails to explain the results of Bridgman's tests (9) which indicate that materials will not yield under a stress condition consisting of purely hydrostatic pressure, that is $\sigma_1 = \sigma_2 = \sigma_3 =$ constant (compression). Another disadvantage of this theory is that the significant number σ_o is the same for tension and compression.

The maximum strain theory postulates that a failure condition is reached at a critical value of strain:

$$\varepsilon = \frac{\sigma_o}{E}$$

If Hooke's Law is valid for the material and the critical stresses for tension and compression are equal, we may state the limiting condition:

$$\left[\left\{\sigma_1 - \nu(\sigma_2+\sigma_3)\right\}^2 - \sigma_o^2\right]\cdot\left[\left\{\sigma_1 - \nu(\sigma_1+\sigma_3)\right\}^2 - \sigma_o^2\right]\cdot\left[\left\{\sigma_3 - \nu(\sigma_2 - \sigma_1)\right\}^2 - \sigma_o^2\right] = 0.$$

However, this theory cannot account for the large strains which occur in a material under hydrostatic pressure without causing failure.

The maximum shear theory regards the critical condition to be caused by the shear stress acting on a plane at 45 degrees to the principal stresses. The significant number for the uniaxial compression test is $\sigma_o/2$ where σ_o is the unconfined compressive strength. This theory neglects

the influence of the stress acting normal to the shear plane; thus, the possibility of shear strength factors, such as internal friction, is ignored. The limiting condition may be expressed:

$$\left[(\sigma_1 - \sigma_2)^2 - \sigma_o^2\right]\cdot\left[(\sigma_1 - \sigma_3)^2 - \sigma_o^2\right]\cdot\left[(\sigma_2 - \sigma_3)^2 - \sigma_o^2\right] = 0 \quad .$$

The maximum octahedral stress theory considers the stresses acting on the octahedral plane. The normal to this plane corresponds to the major diagonal of a cube where the sides of the cube represent the three principal stress planes; thus, the direction cosines of this normal are $\pm 1/\sqrt{3}$ with respect to the directions of the principal stresses. the significant number is $0.47\ \sigma_o$ where σ_o is the unconfined compressive strength, and the limiting condition,

$$(\sigma_1 - \sigma_2)^2 + (\sigma_2 - \sigma_3)^2 + (\sigma_3 - \sigma_1)^2 - 2\sigma_o^2 = 0 \quad ,$$

likewise neglects the influence of the normal stress acting on the shear plane.

The maximum energy theory considers the energy per unit volume of an elastic solid which may be expressed as:

$$\omega = \frac{1}{2E}\left(\sigma_1^2 + \sigma_2^2 + \sigma_3^2\right) - \frac{\nu}{E}\left(\sigma_1\sigma_2 + \sigma_1\sigma_3 + \sigma_2\sigma_3\right) \quad .$$

The significant number is the specific energy, $\frac{\sigma_o^2}{2E}$, for the uniaxial compression and the limiting condition is:

$$\left(\sigma_1^2 + \sigma_2^2 + \sigma_3^2\right) - 2\nu\left(\sigma_1\sigma_2 + \sigma_2\sigma_3 + \sigma_1\sigma_3\right) - \sigma_o^2 = 0 \quad .$$

This theory also fails to explain the capacity of material to withstand a high hydrostatic state of stress without yielding.

The maximum energy of distortion theory regards the influence of change of shape rather than total energy of volume change. The significant number $\left(\frac{1+\nu}{3E}\right)\sigma_o^2$, is obtained by subtracting the energy of volume change from the total elastic energy as measured in the uniaxial test. The limiting condition is:

$$\left(\sigma_1 - \sigma_2\right)^2 + \left(\sigma_2 - \sigma_3\right)^2 + \left(\sigma_3 - \sigma_1\right)^2 - 2\sigma_o^2 = 0 \quad ,$$

which is identical to the octahedral stress theory.

Mohr's Theory of Strength (25)

Nadai (25), p. 214, describes Mohr's theory with the following statement:

> A material may fail either through plastic slip or by fracture when either the shearing stress τ in the planes of slip has increased to a certain value which in general will depend also on the normal stress σ acting across the same planes or when the largest tensile normal stress has reached a limiting value dependent on the properties of the material.

Fine traces of slip lines can be seen on the surface of test specimens of polycrystalline ductile metals and rocks which have been deformed beyond the elastic limit. The slip lines meet at a constant angle and are inclined with respect to the direction of the principal stresses. It has been observed that the direction of the algebraically larger principal stress bisects the acute angle between the directions of slip. It has been further noted, according to Nadai, that brittle crystalline materials such as cast iron, rocks, or concrete, when subjected to uniaxial compression, always fracture at an angle with the

vertical (in this case, also the direction of the major principal stress) of less than 45°.

According to Mohr the shearing stress in the plane of slip is solely a function of the normal stress acting on this surface. If a coordinate system of shearing stress and normal stress is constructed, a curved line representing $\tau = f(\sigma)$ may be drawn as found experimentally. Also, on this coordinate system, Mohr's stress circles may be drawn for various values of principal stresses. Mohr further postulates that the intermediate principal stress is without influence in contributing to failure since its direction is mutually perpendicular to the direction of slip and the direction of the normal stress on the slip plane. If this is true, then only the circles representing σ_1 and σ_3 need be constructed. The largest of these circles that can be drawn is the circle which is tangent to the curve $\tau = f(\sigma)$. A larger circle would indicate possible shear and normal stress values which were larger than the experimental fact. The curve $\tau = f(\sigma)$ then represents the envelope of the largest principal stress circles. It is further postulated that the coordinates at the point of tangency represent the critical combination of shear and normal stress for slip, hence, fracture. The angle between the slip planes can be measured from the limiting principal stress circle, which is the angle between the radius passing through the point of tangency and the normal stress axis. It may also be shown that the radius of the largest principal stress circle is a function of the distance from the origin to the center of the circle which is expressed:

$$1/2(\sigma_1 - \sigma_3) = F\left(1/2(\sigma_1 + \sigma_3)\right) \quad .$$

The above function is also the locus of maximum shear stress (see Figures 23 - 26). If we denote

$$p = 1/2(\sigma_1 + \sigma_3) \quad ,$$

and

$$\tau_m = 1/2(\sigma_1 - \sigma_3) \quad ,$$

we may write

$$\tau_m = F(p)$$

and substituting into the general expression for Mohr's stress circle we have:

$$(\sigma - p)^2 + \tau^2 = \tau^2_m$$

which is the parametric form of the family of principal stress circles.

The Octahedral Shear Stress Theory for Fracture (17, 22, 29)

The general equations of the limiting condition and the significant number for the maximum octahedral shear stress theory have already been discussed. This theory was developed primarily to overcome the mathematical difficulties presented in Mohr's theory in formulating the conditions of flow in ductile materials. Hencky (17) included the effect of the intermediate principal stress on flow which is neglected by the Mohr theory and the maximum shearing stress (Tresca) theory. These latter theories may be represented geometrically by "hexagonal"

prisms having axes corresponding to the normal on the octahedral plane. The Hencky-Mesis (22) criterion is represented by a circular cylinder which circumscribes the above mentioned hexagonal prism thus having points in common with the other two theories. One of these common points, corresponds to the conditions of the triaxial shear test.

The Hencky-Mesis theory may be extended such that the octahedral shearing stress is a function of octahedral normal stress (29). One geometric representation would be a circular cone with its axis corresponding to the diagonal $\sigma_1 = \sigma_2 = \sigma_3$. The limiting condition for such a surface would be (see Nadai p. 227):

$$(\sigma_1 - \sigma_2)^2 + (\sigma_2 - \sigma_3)^2 + (\sigma_3 - \sigma_1)^2 = 2/3 \left[c_o(\sigma_1 + \sigma_2 + \sigma_3) - c_1\right]^2$$

where

$$c_o = \frac{\sigma_c - \sigma_t}{\sigma_c + \sigma_t} ,$$

$$c_1 = \frac{2\sigma_c \sigma_t}{\sigma_c + \sigma_t} ;$$

σ_c and σ_t are the yield stress in simple compression and simple tension.

Nadai also developes the limiting conditions for a paraboloid which leads to the possibility that the theory could be extended to any surface of revolution.

The Griffith Theory (12)*

Molecules have an attraction to each other which decreases rapidly

*The following is a summary of Griffith's paper. These ideas are now recognized as an over simplified view of molecular behavior but is of interest because of its wide use in fracture studies.

as separation distance increases. They also possess translation and rotational vibrations which are derived from the thermal energy of the substance. Molecular orientation also influences the attractive forces between molecules. Under suitable conditions, molecules will orient themselves so that they are in a condition of minimum potential energy resulting in a alignment of their axes of maximum attraction. This alignment causes the formation of chains or sheets of molecules which may be straight or curved. It is possible then to expect groups of these oriented molecules to appear as units or cells; the cells, however, have a random orientation. The molecules of an individual cell have greater resistance to rotation than to translation in the direction of the preferred alignment. Crystalline solids generally exhibit molecular sheets which are plane.

These surfaces existing in crystalline materials undergo a mutual sliding when subjected to a sufficiently large shearing force through a distance equal to some integral multiple of molecular spacing without changing the fundamental structure of the crystal. This occurs in conjunction with the yielding of the crystalline lattice structure and the deformation takes place on the "glide planes" or slip surfaces. These slip surfaces may also be considered the surfaces of least molecular attraction. As the crystal surfaces slide from an initial position of stable equilibrium to a second position of equilibrium they must pass through an unstable position. The energy required to cause passage from one stage to another represents the shear strength of the material. This energy will depend upon the molecular force fields. A polycrystalline material which has crystals

oriented at random will have an aggregate shear strength higher than the individual crystal shear strength.

The molecular cohesion must become less as crystal surfaces move on the glide planes and in some instances becomes zero before equilibrium is again reached. If molecular cohesion is lost, then a shear fracture will result unless the specimen is under a sufficiently high confining pressure. A crystalline material, therefore, may behave as a brittle or ductile material depending upon its state of stress. Brittle fracture, according to this theory, may always be prevented by sufficiently high confining pressures and an axial load of sufficient magnitude to cause shear failure.

Molecules in a single crystal are thought of as being in a condition of maximum stability with the interior molecules more stable than those at the boundary of the crystal. The molecules of least stability will tend to rotate in the presence of a shear force; this rotation is strongly resisted by forces of a viscous nature dependent on the amount and duration of the applied stress. This phenomenon, when occurring over a long period of time, is termed elastic after working. Experiments have shown, however, that this property belongs to crystalline materials and not to single crystals.

Griffith further considers two adjacent crystals, separated by a plane boundary, sliding with respect to each other. There are only a finite number of stable positions available to the crystals with an infinite number of intervening unstable positions. If these two crystals are imbedded in a number of others the boundary molecules of both crystals will be pulled in the direction of the nearest stable position

thus placing a strain in the material. At a certain value of shearing stress, these crystals will undergo a relative displacement. The boundary molecules will be pulled away and, after passing through unstable positions, will assume new positions and their original stability be restored. After the load is removed, these molecules will remain in their new position since, in order to regain the original position, they must pass through a condition of instability or maximum potential energy. A shear force of opposite sense would be required to reverse a movement.

A crystal having a random orientation in a polycrystalline material or embedded in an amorphous material is changed structurally when yielding occurs. The interior of the crystal remains the same but the less stable boundary molecules are extremely distorted and add to the number of molecules which possess inferior stability. As a result of this, an amorphous layer of appreciable thickness is generated on the slip surfaces.

For very large strains the shear force must be resisted by amorphous boundary layers. If the amorphous layers have considerable shear strength compared with the shear strength of the original material, the undeformed material is regarded as ductile. The formation of non-crystalline material at intercrystalline boundaries explains the sudden drop in shear strength in ductile metals occurring immediately after yield.

Griffith also explains the influence of strain rate on shear strength by stating that a mutual surface tension, existing between crystals at the crystalline boundaries, is reduced if the transition between crystals is gradual. Reduction of surface tension is attributed to the lowering of the surface energy of crystals due to the build up of amorphous layers. Because the surface energy is lowered, the stress required to maintain deformation after yield is lower than the stress required for yield.

Griffith concludes that the molecular orientation theory can, in general, explain the phenomena relating to the mechanical properties of all solids. Also, the conditions for flow of brittle materials under triaxial stress may be explained by the molecular orientation theory.

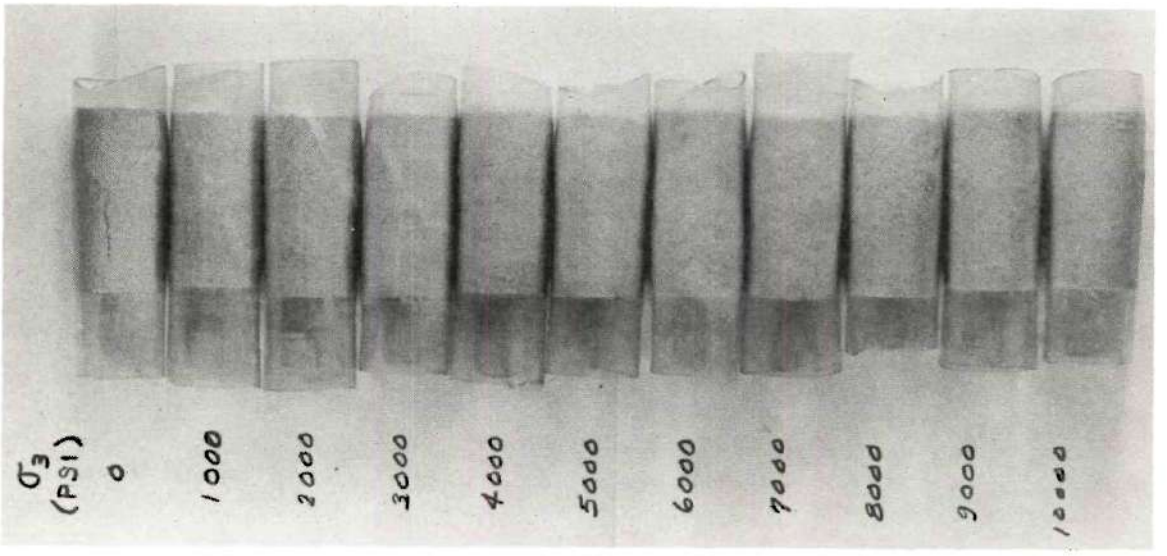

Figure 10. Failure Planes for Indiana Limestone.

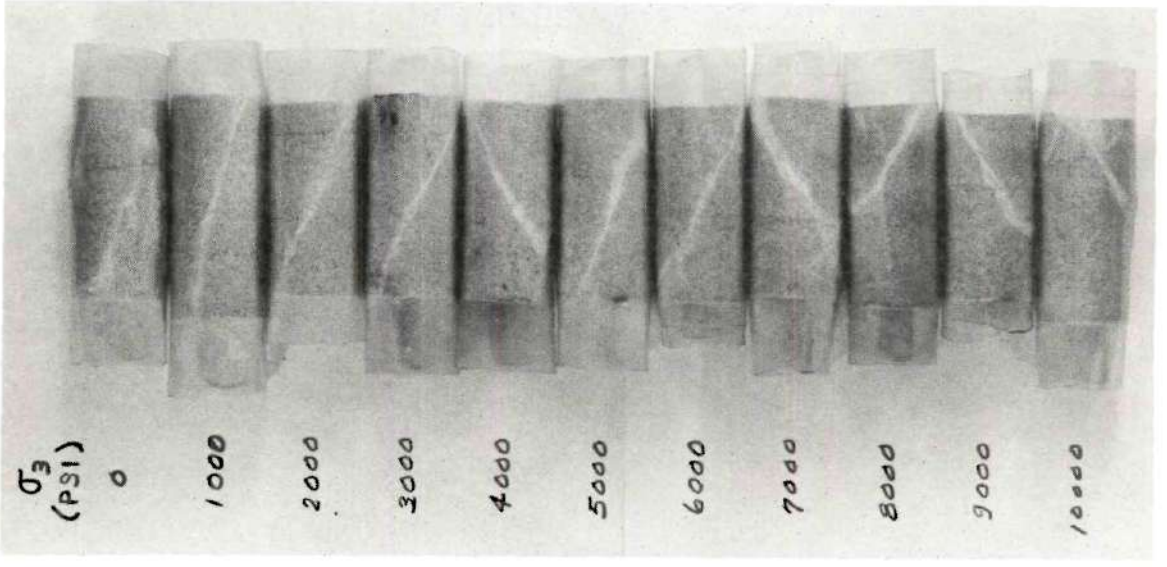

Figure 11. Failure Planes for Potsville Sandstone.

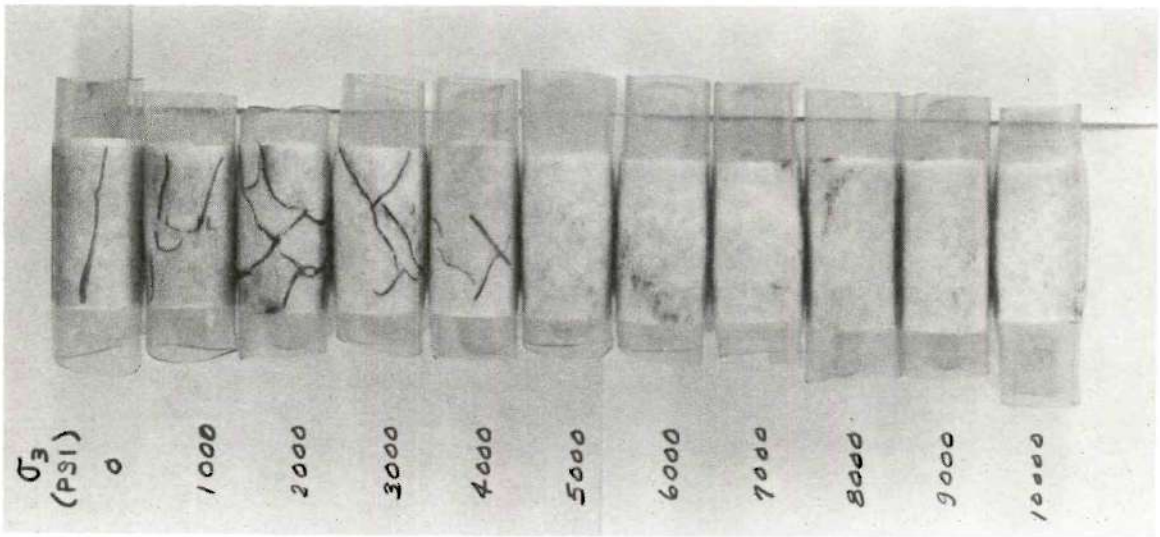

Figure 12. Failure Planes for Georgia Marble.

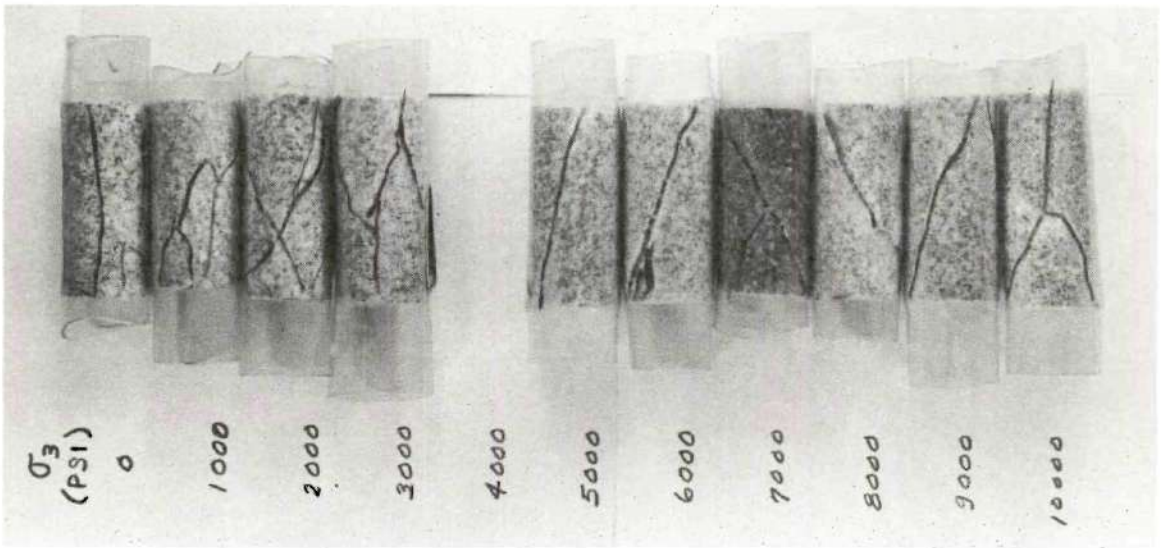

Figure 13. Failure Planes for Stone Mountain Granite.

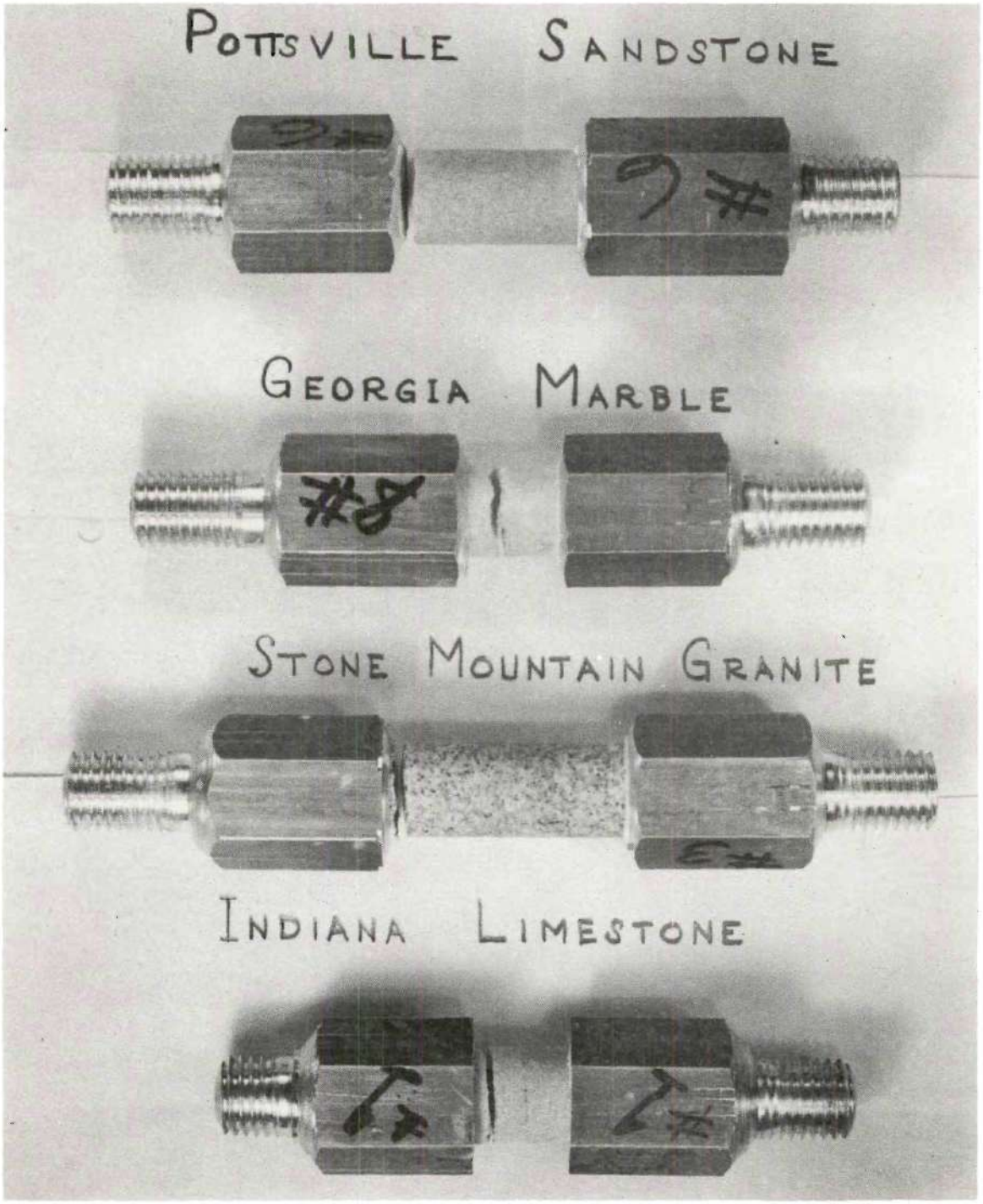

Figure 14. Failure Planes for Tension Tests.

Figure 15a. Cross-section of Indiana Limestone Core Before Test. (50x).

Figure 15b. Shear Surface of Indiana Limestone Core After Test. (50x).

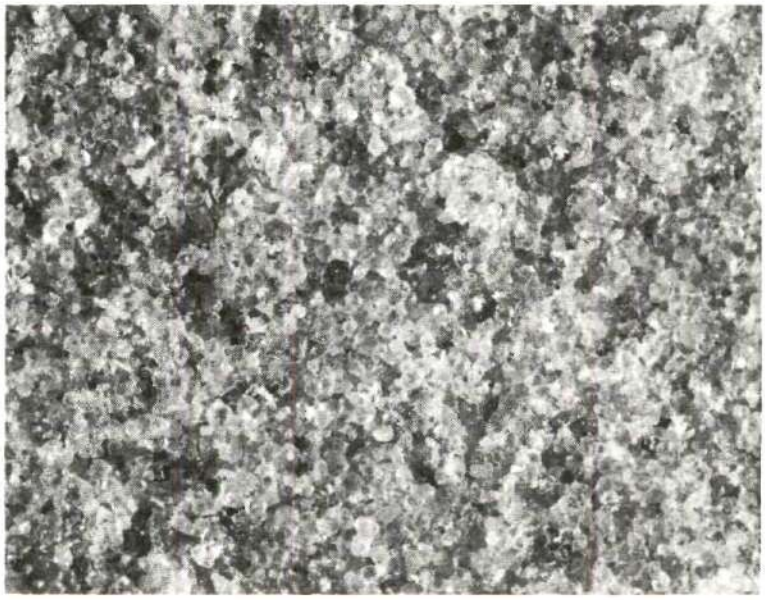

Figure 16a. Cross-section of Potsville Sandstone Core Before Test. (50x).

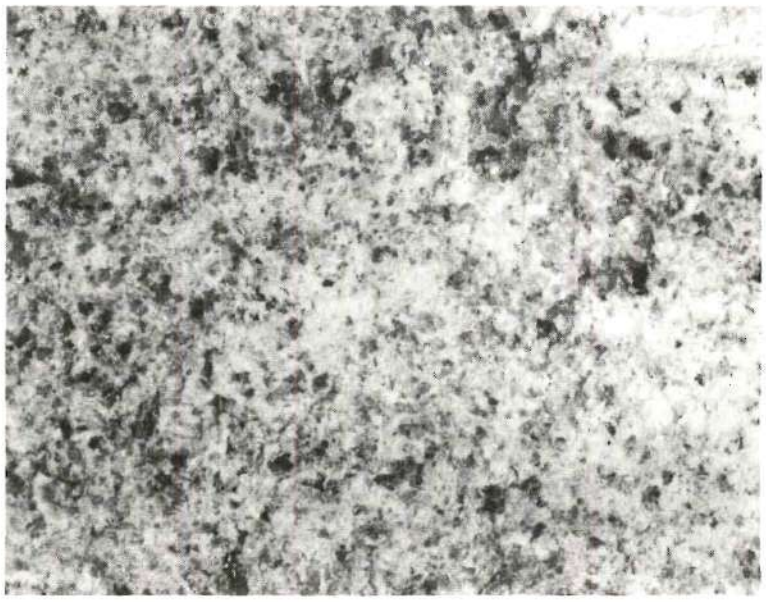

Figure 16b. Shear Surface of Potsville Sandstone Core After Test. (50x).

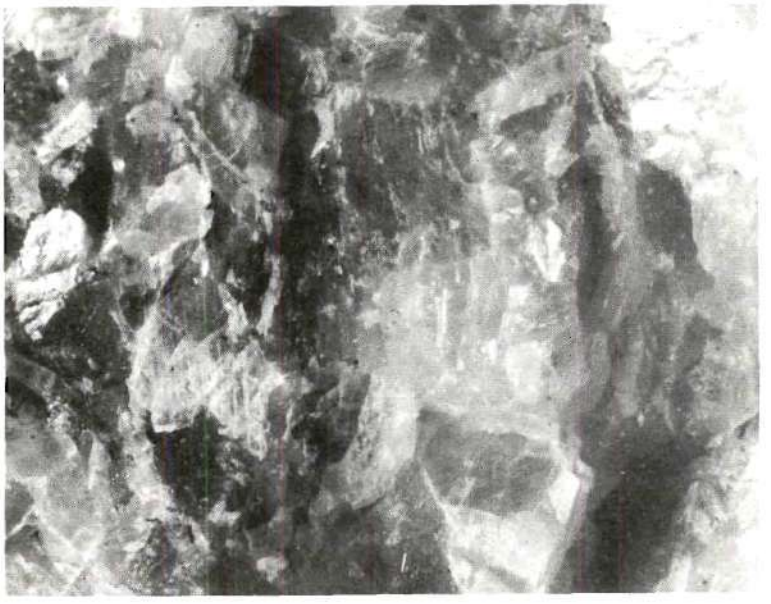

Figure 17a. Cross-section of Georgia Marble Core Before Test. (50x).

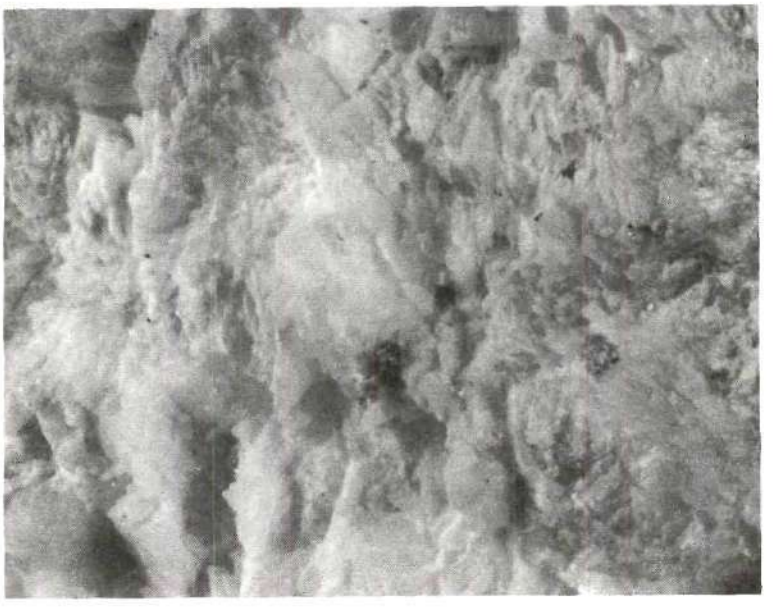

Figure 17b. Shear Surface of Georgia Marble Core After Test. (50x).

Figure 18a. Cross-section of Stone Mountain Granite Before Test.

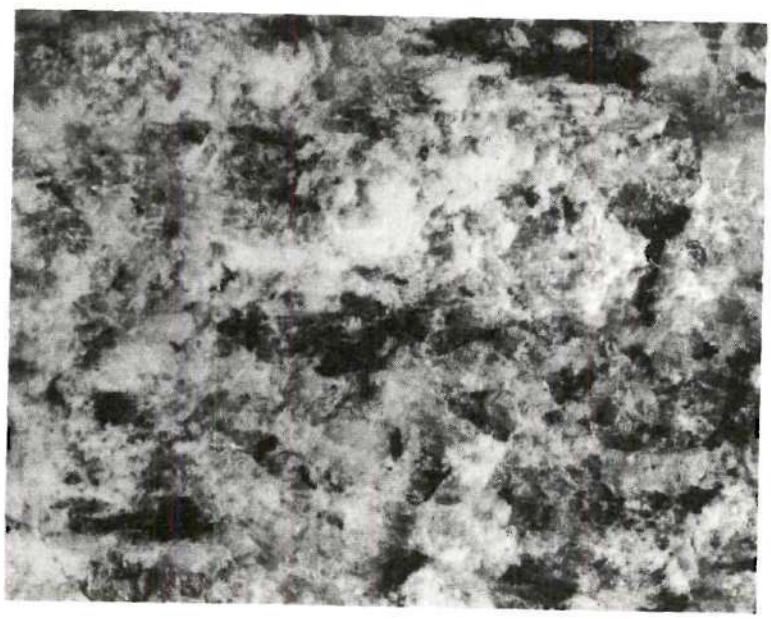

Figure 18b. Cross-section of Stone Mountain Granite After Test.

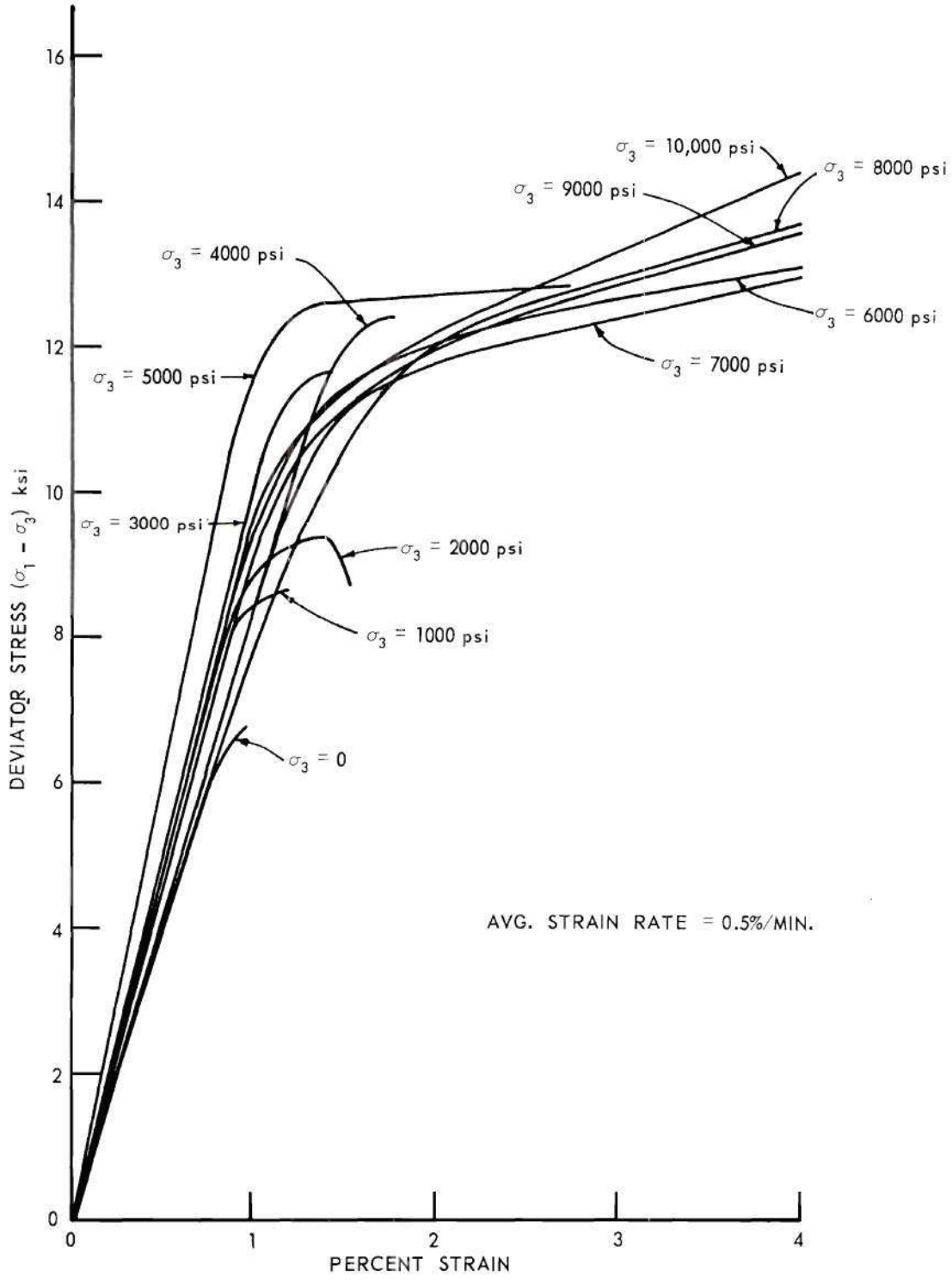

Figure 19. Stress-strain Curves for Indiana Limestone.

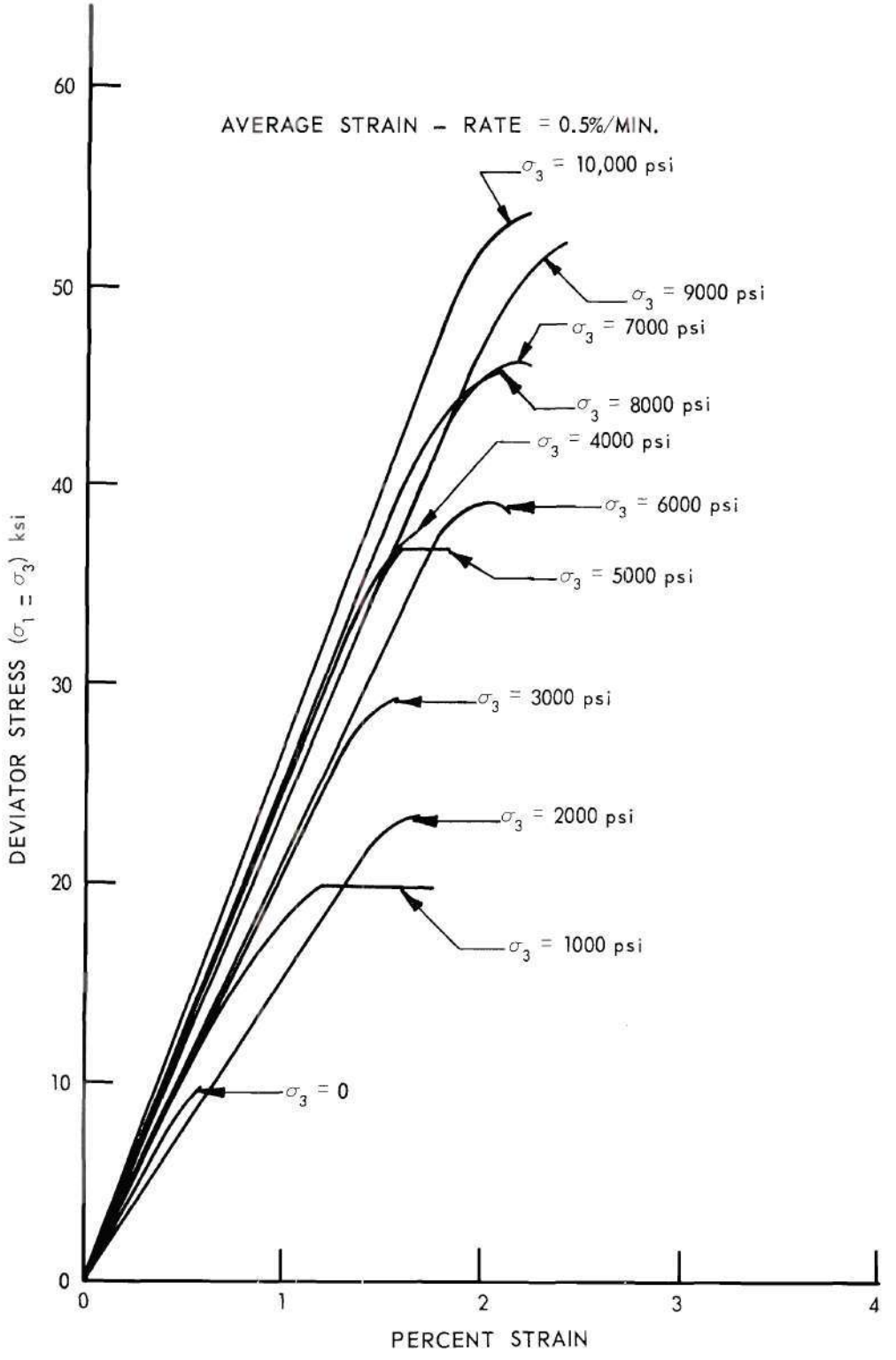

Figure 20. Stress-strain Curves for Potsville Sandstone.

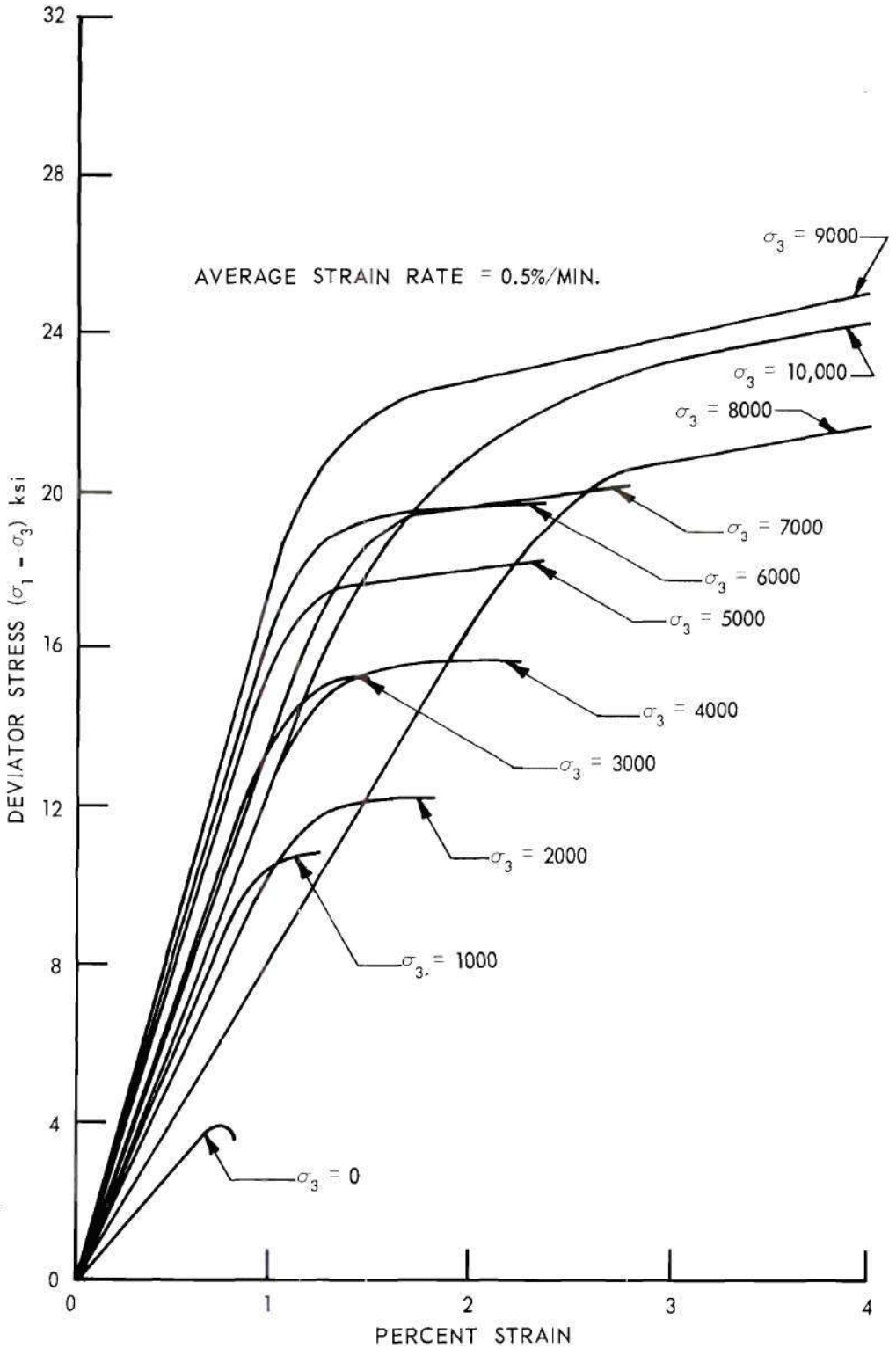

Figure 21. Stress-strain Curves for Georgia Marble.

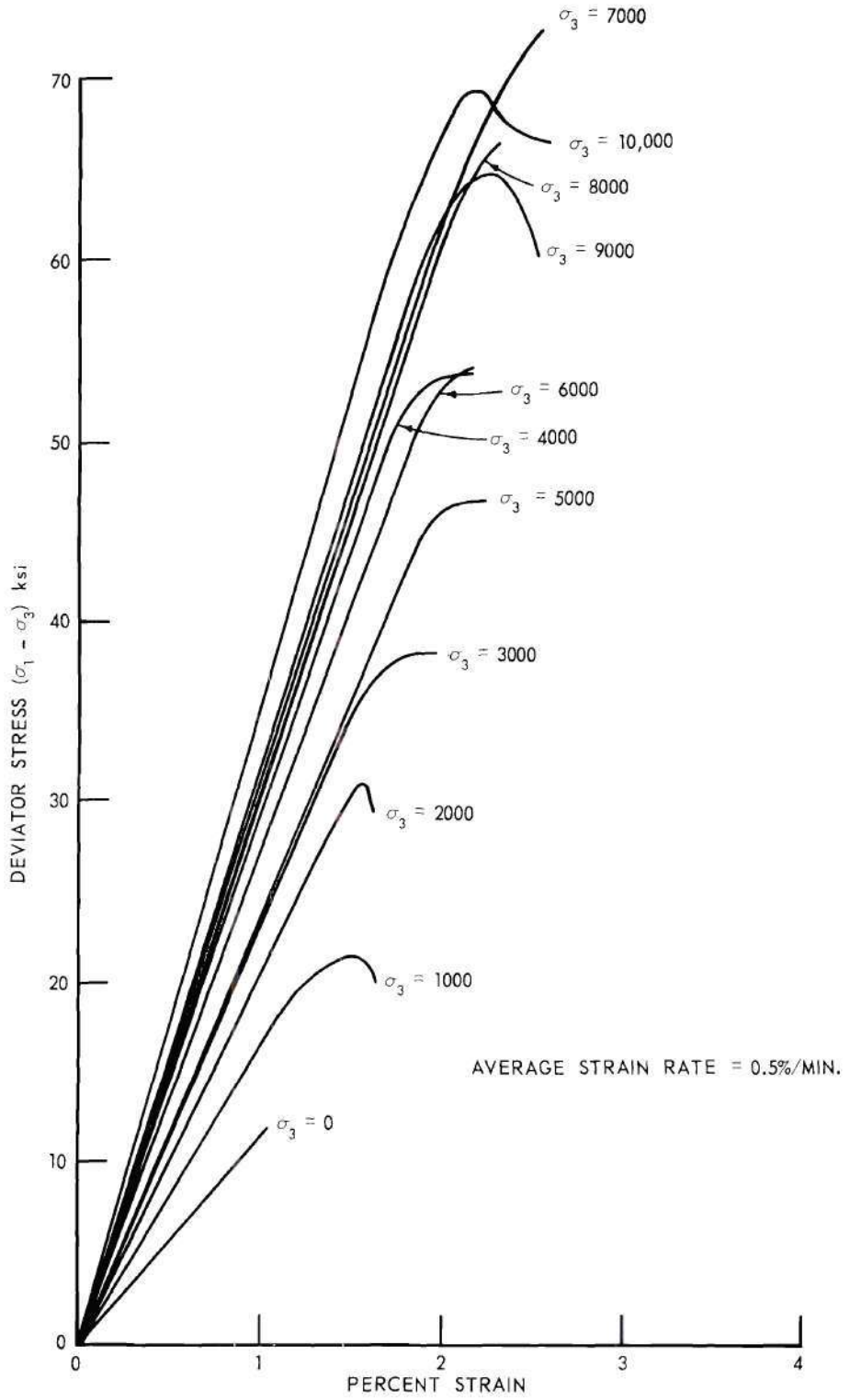

Figure 22. Stress-strain Curves for Stone Mountain Granite.

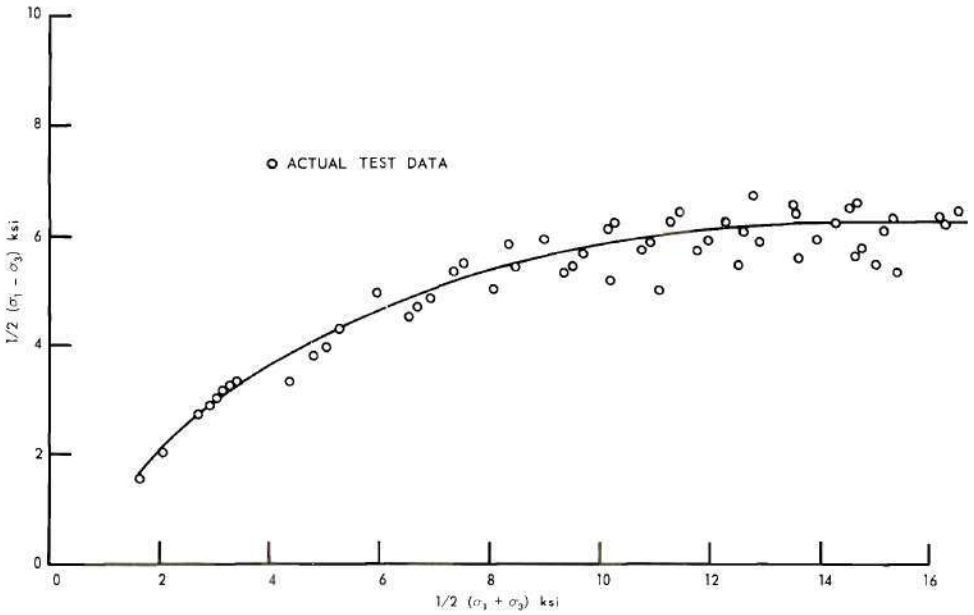

Figure 23. Indiana Limestone Test Results.

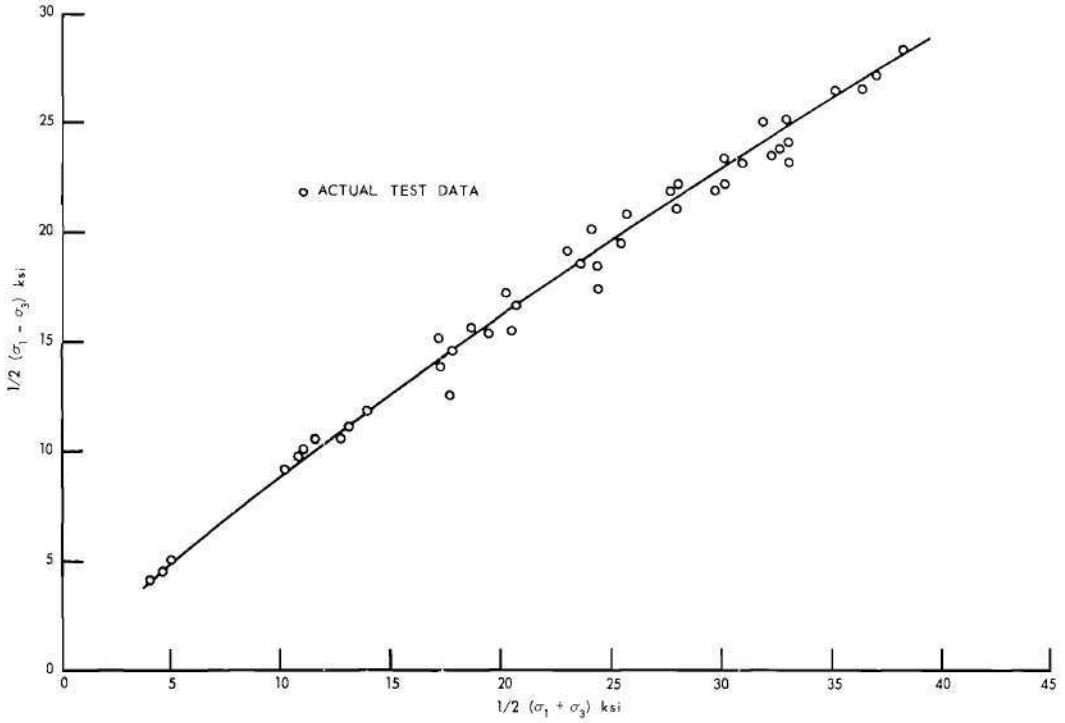

Figure 24. Potsville Sandstone Test Results.

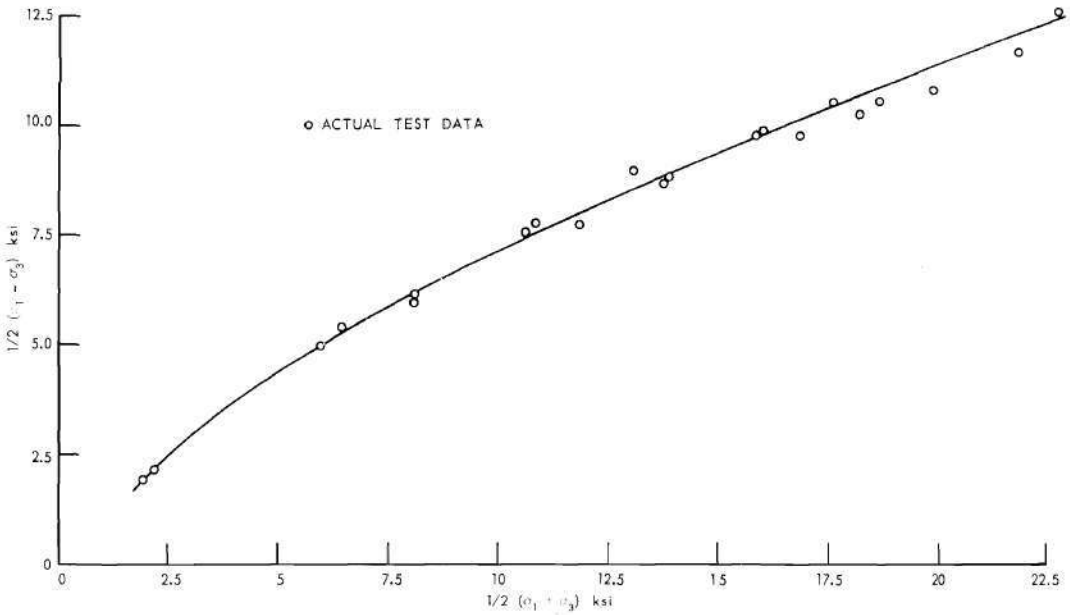

Figure 25. Georgia Marble Test Results.

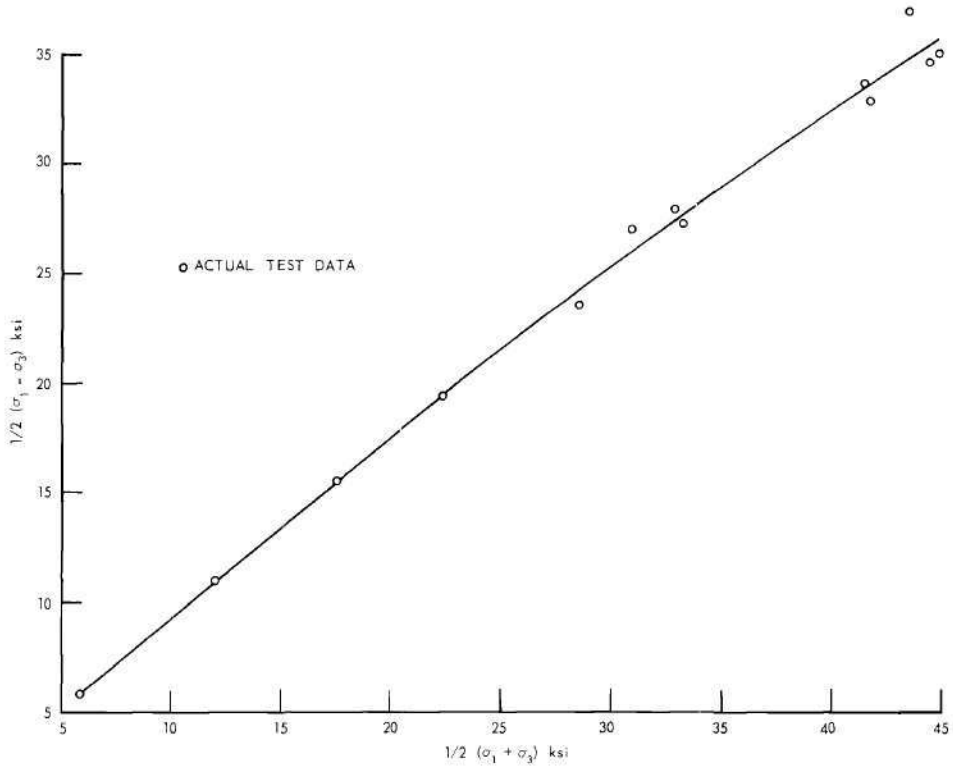

Figure 26. Stone Mountain Granite Test Results.

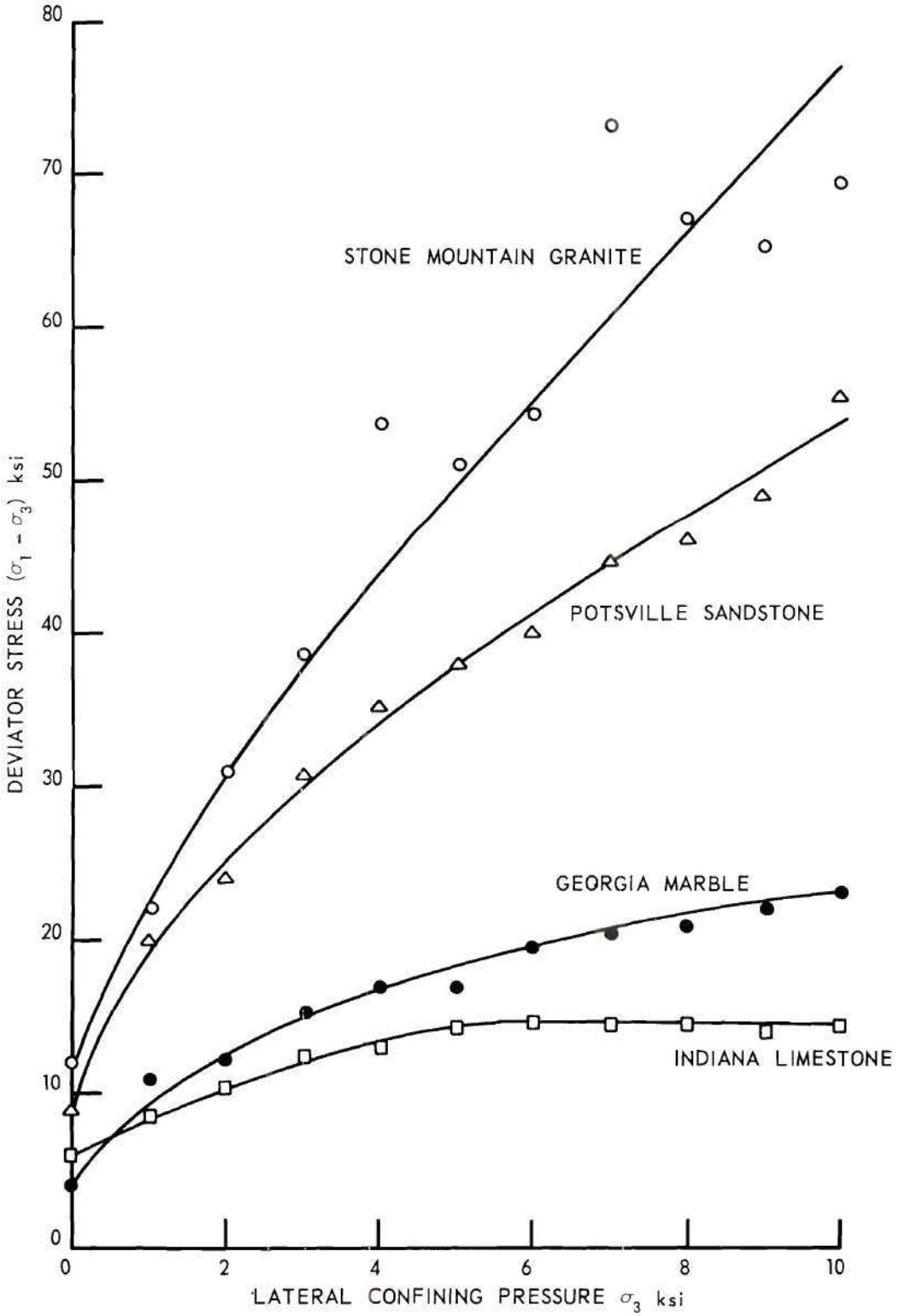

Figure 27. Deviator Stress vs. Confining Pressure.

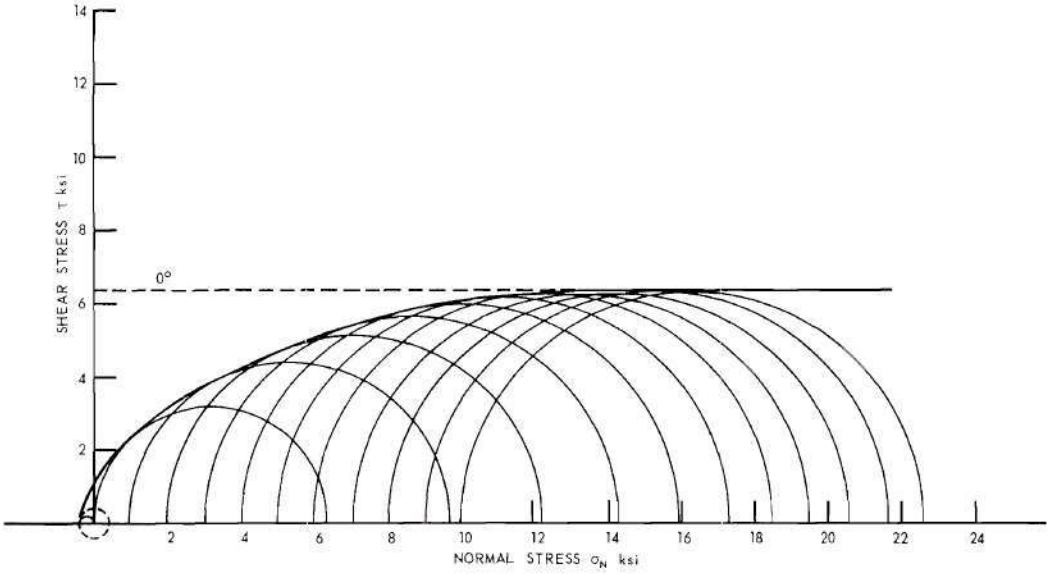

Figure 28. Mohr's Circles for Indiana Limestone.

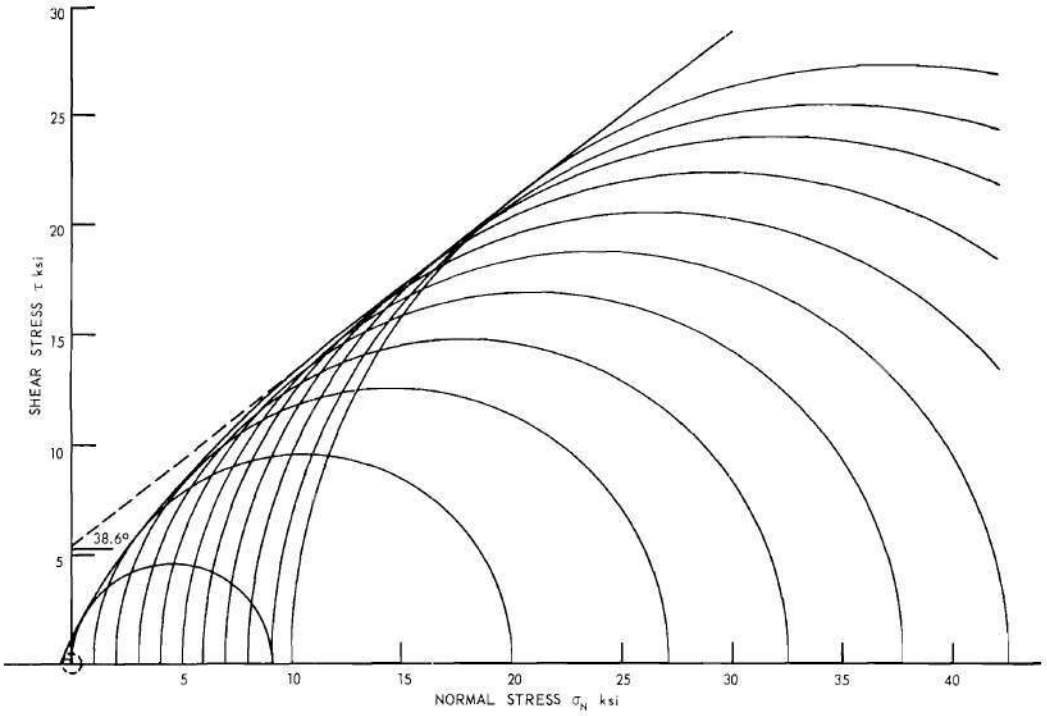

Figure 29. Mohr's Circles for Potsville Sandstone.

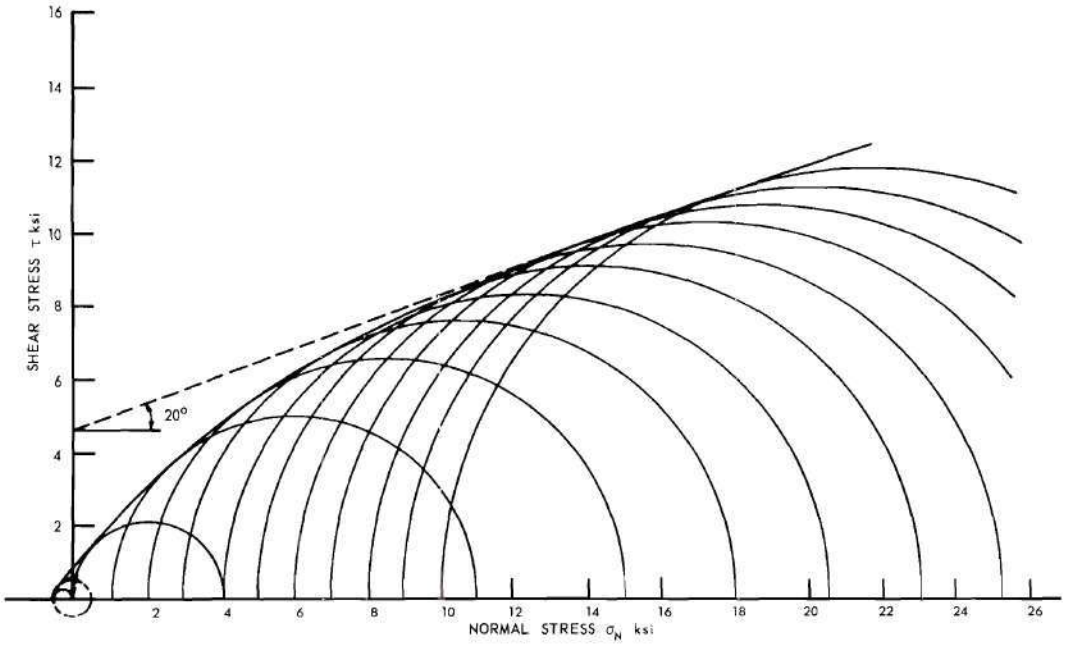

Figure 30. Mohr's Circles for Georgia Marble.

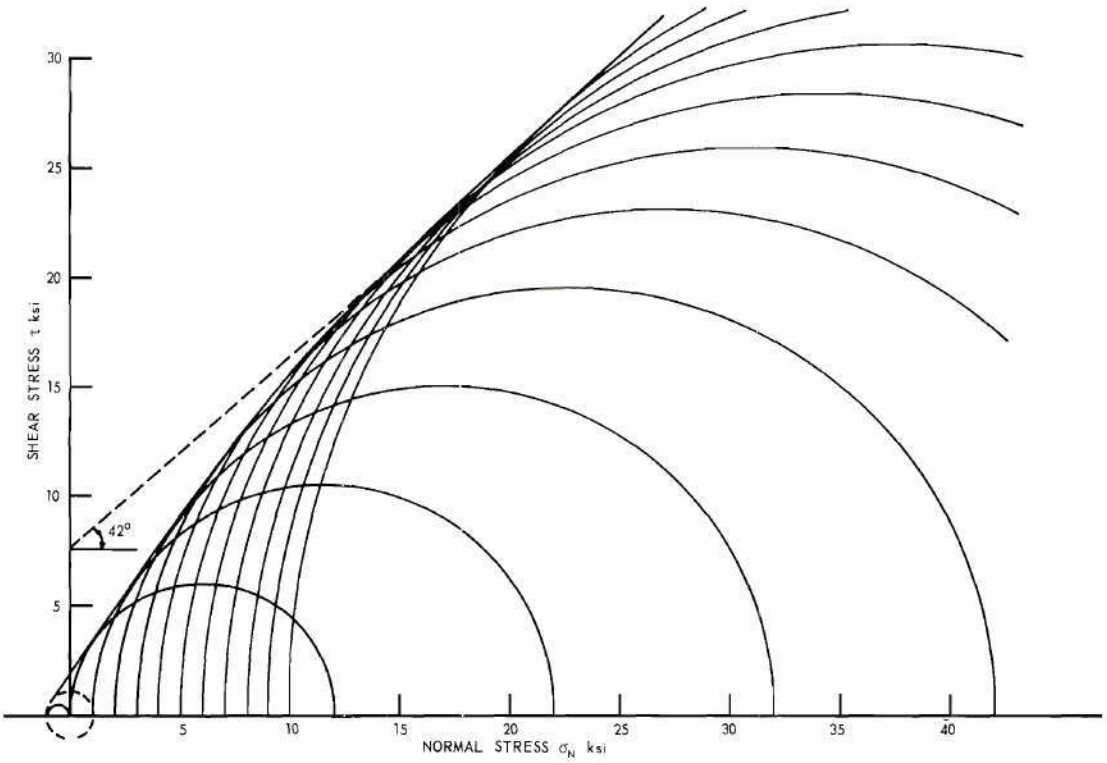

Figure 31. Mohr's Circles for Stone Mountain Granite.

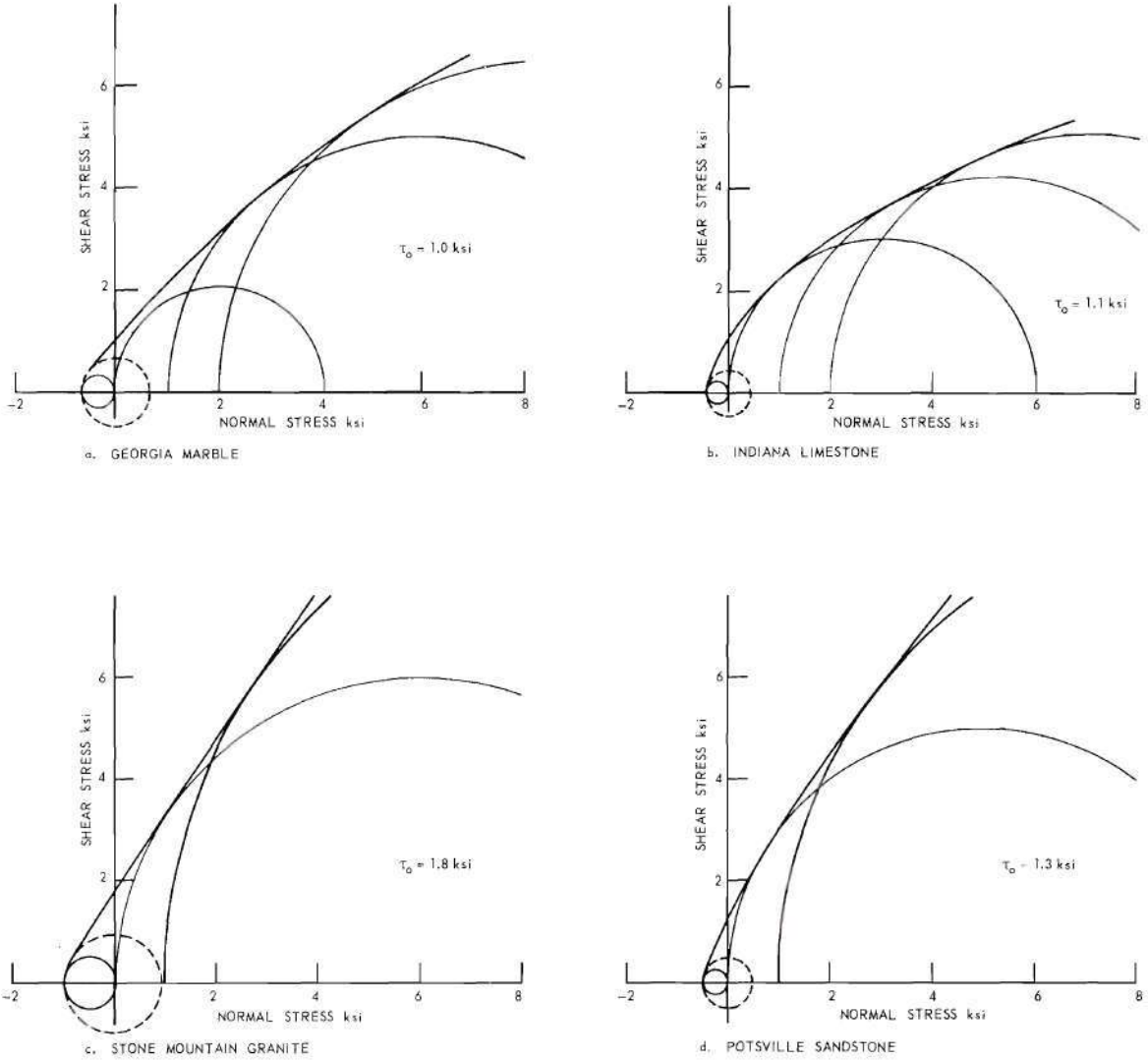

Figure 32. Determination of the Shear Intercept.

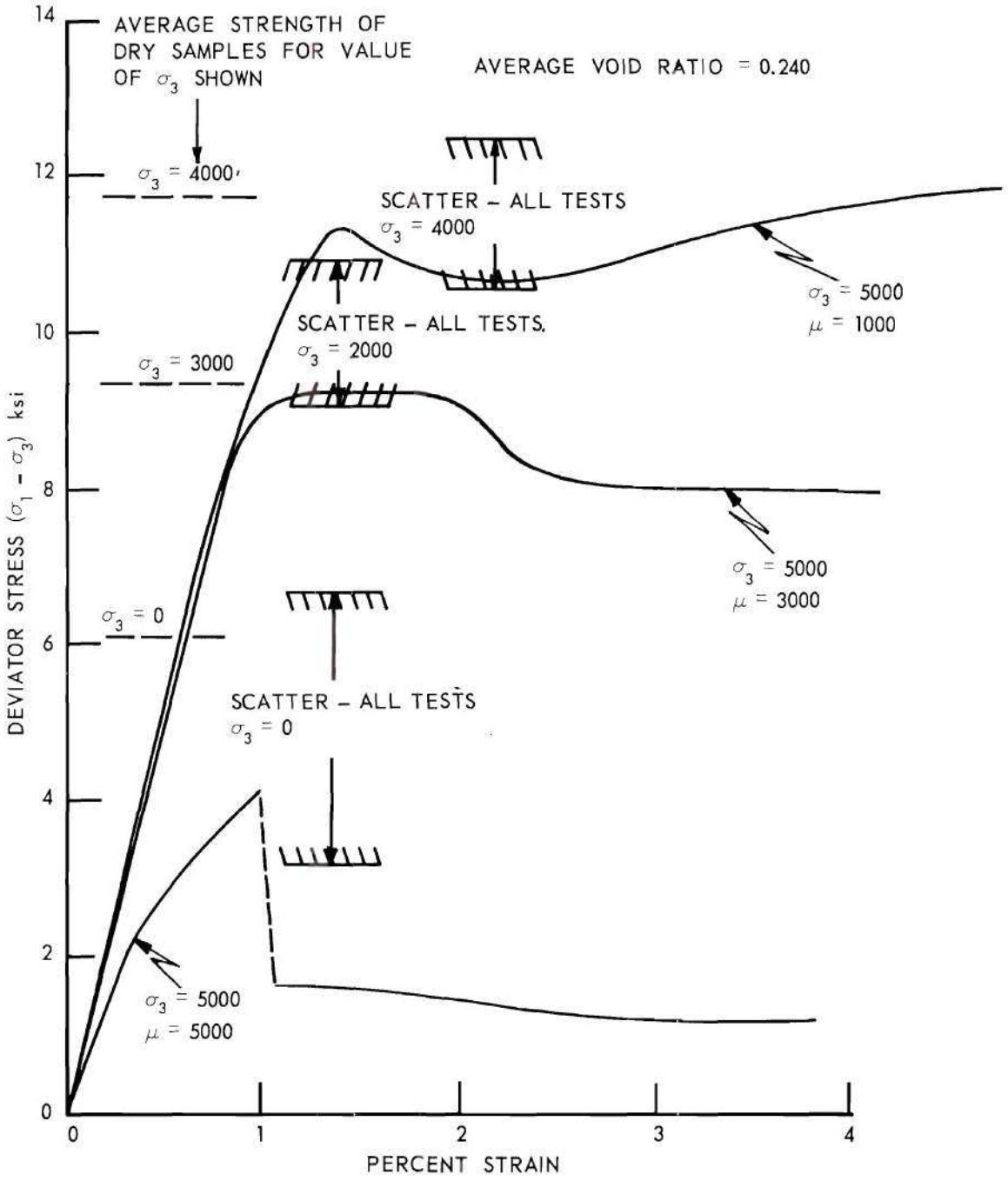

Figure 33. Pore Pressure Tests for Indiana Limestone.

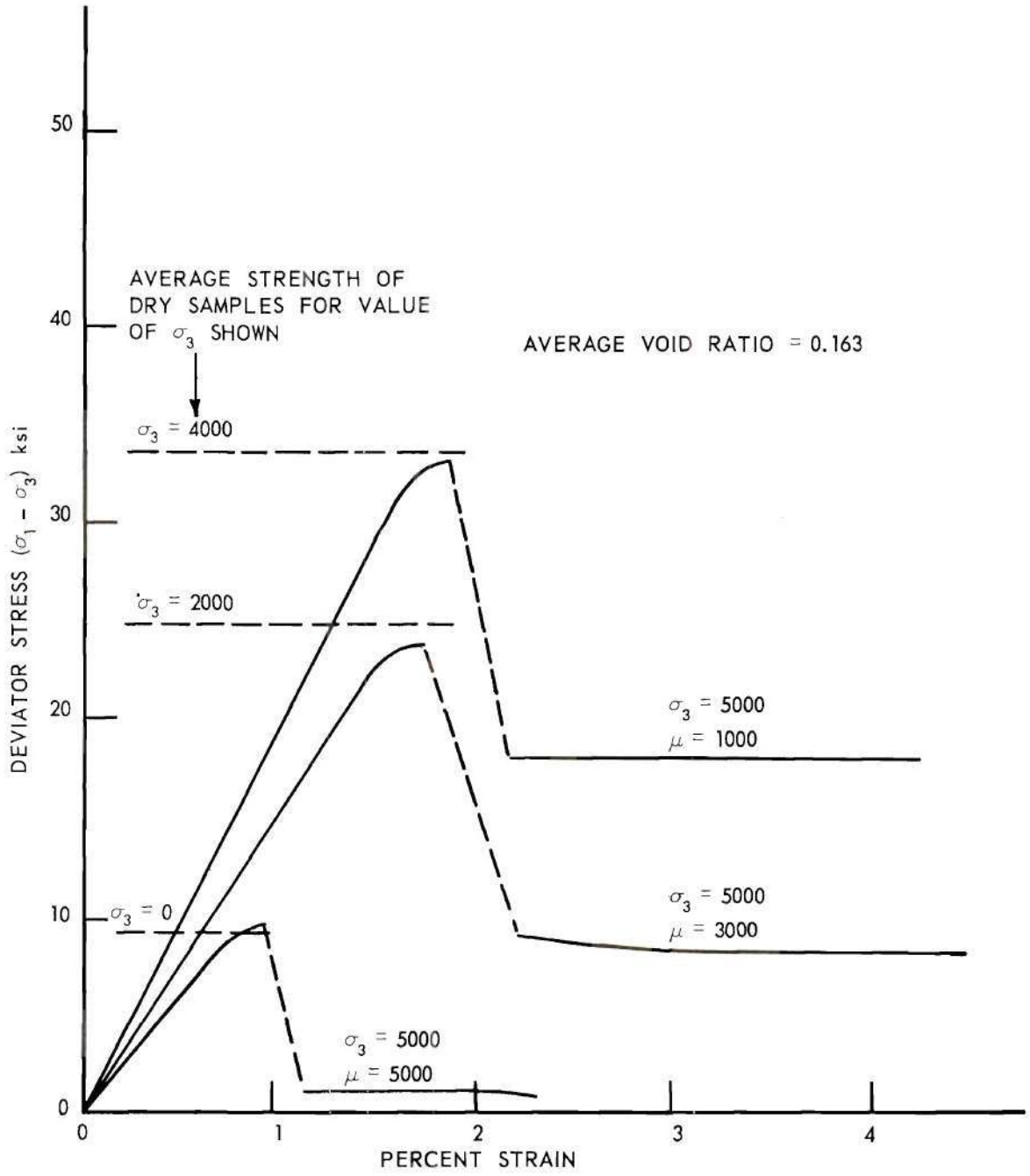

Figure 34. Pore Pressure Tests for Potsville Sandstone.

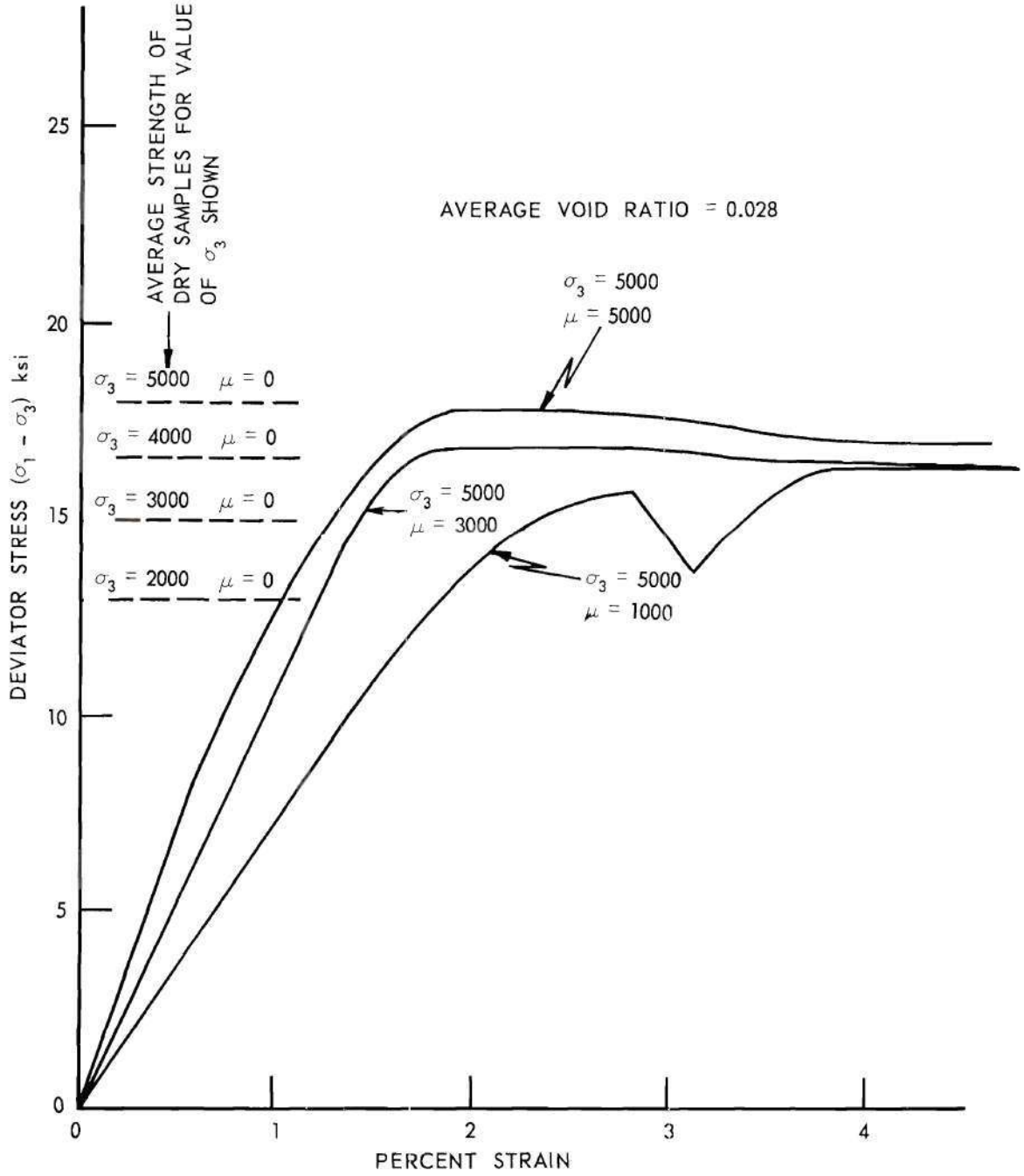

Figure 35. Pore Pressure Tests for Georgia Marble.

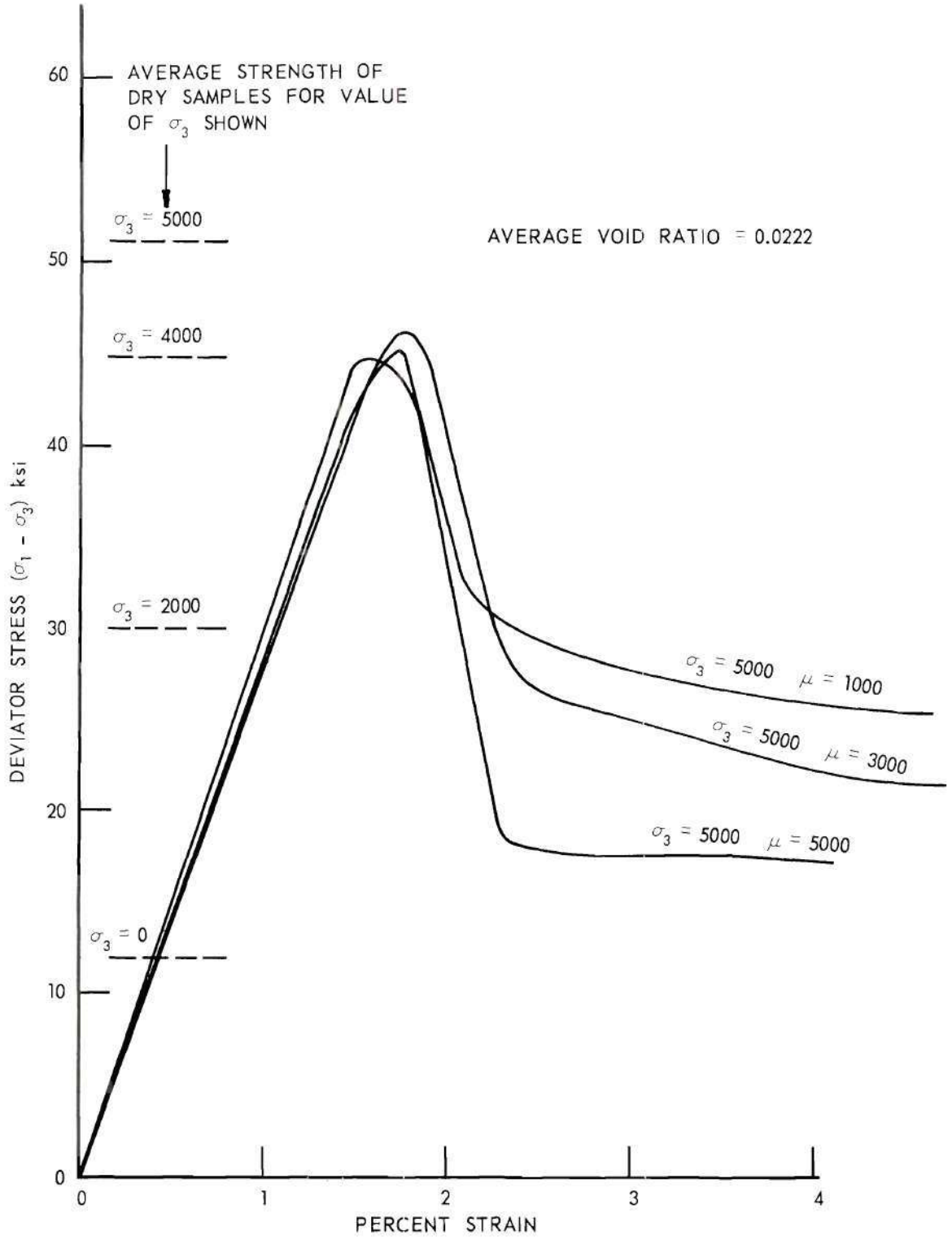

Figure 36. Pore Pressure Tests for Stone Mountain Granite.

BIBLIOGRAPHY

LITERATURE CITED

(1) F. D. Adams and J. T. Nicholson, "An Experimental Investigation into the Flow of Marble", Philosophical Transactions of the Royal Society of London, 1901, pp. 363-401.

(2) F. O. Anderegg, "Efflorescence and Staining of Indiana Limestone", Purdue Engineering Experimental Station Report, no. 33 pp. 8-11.

(3) L. V. Azaroff, Introduction to Solids, McGraw-Hill Book Company, New York, 1960, 459 pp.

(4) G. G. Balmer, "Physical Properties of Some Igneous Rocks", U. S. Bureau of Reclamation Concrete Laboratory Report, no. sp-39, 1953, pp. 1-15.

(5) R. F. Blanks and D. McHenry, "Large Triaxial Testing Machine Built by the Bureau of Reclamation", Engineering News Record, vol. 171, 1945, pp. 113-115.

(6) R. Böker, "Die Mechanik der bleibenden Formänderungen in kristallinische aufgebauten Körpern", Mitteilungen über dem Vereines deutscher Ingenieure, vol. 175, 1915, p. 1.

(7) H. Borowicka, "Soil Mechanics-Rock Mechanics", Mitteilungen des Institutes für Grundbau und Bodenmechanik, Viena, 1962, pp. 3-11.

(8) R. O. Bredthauer, "Strength Characteristics of Rock Samples under Hydrostatic Pressure", Transactions of the American Society of Mechanical Engineers, 1957, pp. 695-708.

(9) P. W. Bridgman, Physics of High Pressure, Macmillan Company, New York, 1931, pp. 70-75.

(10) P. W. Bridgman, Studies in Large Plastic Flow and Fracture, McGraw-Hill Book Company, New York, 1952, p. 111, p. 123.

(11) D. P. Clausing, "Comparison of Griffith's Theory and Mohr's Failure Criteria", Third Symposium on Rock Mechanics, Golden, Colorado, 1959, pp. 285-296.

(12) A. A. Griffith, "The Phenomena of Rupture and Flow in Solids", Philosophical Transactions of the Royal Society of London, vol. 221, 1921, pp. 183-198.

(13) D. T. Griggs, "Deformation of Rocks under High Confining Pressures", The Journal of Geology, vol. 44, 1936, pp. 541-577.

(14) J. Handin, "Strength and Plasticity", Shell Development Company, Exploration and Production Research Publication, no. 99, 1956, pp. 1-15.

(15) J. Handin, "An Application of High Pressure in Geophysics: Experimental Rock Deformation", Transactions of the ASME, vol. 75, 1953, pp. 315-324.

(16) J. Handin and R. V. Hager, Jr., "Experimental Deformation of Sedimentary Rocks under Confining Pressure: Tests at Room Temperature on Dry Samples", Bulletin of the American Association of Petroleum Geologists, vol. 41, 1957, pp. 1-50.

(17) H. Hencky, "Über das Wesen der plastischen Verformung", Zeitschrift des Vereines deutscher Ingenieure, vol. 69, 1925, p. 695.

(18) M. J. Hvorslev, "Physical Components of the Shear Strength of Saturated Clays", American Society of Civil Engineers Research Conference on Shear Strength of Cohesive Soils, Boulder, Colorado, 1960, pp. 169-273.

(19) H. Jeffreys, The Earth, Cambridge University Press, London, 1924, p. 111.

(20) T. von Kármán, "Festigkeitsversuche unter allseitigem Druck", Zeitschrift des Vereines deutscher Ingenieure, vol. 55, no. 42, 1911, pp. 1749-1757.

(21) T. W. Lambe, "A Mechanistic Picture of Shear Strength in Clay", ASCE Research Conference on Shear Strength of Cohesive Soils, Boulder, Colorado, 1960, pp. 555-580.

(22) R. von Mises, "Mechanik der festen Körper im plastisch-deformablen Zustand", Nachrichten technische Gesellschaft Wissenschaft Göttingen, Mathematik-physik Klasse, 1913.

(23) O. Mohr, Abhandlungen aus dem Gebiete der technischen Machanik, 2nd ed., W. Ernst und Sohn, Berlin, 1914, pp. 192-235.

(24) D. G. Moye, "Rock Mechanics in the Investigation and Construction of T.1 Underground Power Station, Snowy Mountains, Australia", Engineering Geology Case Histories, no. 3, Symposium on Rock Mechanics, The Geological Society of America, St. Louis, Missouri, 1958, p. 26.

(25) A Nadai, Theory of Flow and Fracture of Solids, McGraw-Hill Book Company, New York, 1950, pp. 572.

(26) E. C. Robertson, "Experimental Study of the Strength of Rock", Bulletin of the Geological Society of America, vol. 66, 1955, pp. 1275-1314.

(27) L. H. Robinson, "The Mechanics of Rock Failure", Third Symposium on Rock Mechanics, Golden, Colorado, 1959, pp. 177-199.

(28) M. Roš and A. Eichinger, "Versuche zur Klärung der Frage der Bruchgefahr. II. Nichtmetallische Stoffe", Eidgenossische Materialprufungsamstalf an der Eidgenossischen Technischen Hochschule, Zurich, 1928, p. 57.

(29) F. Schleicher, "Der Spannungszustand an der Fliessgrenze", Zeitschrift für angewandte Mathematik und Mechanik, vol. 6, 1926, p. 216.

(30) S. Serata, "Transition from Elastic to Plastic States of Rocks under Triaxial Compression", Fourth Symposium on Rock Mechanics, Pennsylvania State University, 1961, 25 pp.

(31) S. Serdengecti and G. D. Boozer, "The Effect of Strain Rate and Temperature on the Behavior of Rocks Subjected to Triaxial Compression", Fourth Symposium on Rock Mechanics, Pennsylvania State University, 1961, 34 pp.

(32) I. K. Silverman, "Behavior of Materials and Theories of Failure", Second Symposium on Rock Mechanics, Golden, Colorado, 1957, pp. 3-17.

(33) K. Terzaghi, Theoretical Soil Mechanics, John Wiley and Sons, New York, 1943, p. 12.

(34) K. Terzaghi, "Stress Conditions for the Failure of Saturated Concrete and Rock", American Society for Testing Materials Proceedings, vol. 45, 1945, pp. 777-801.

(35) A. D. Topping, "The Use of Experimental Constants in the Application of Theories of Strength to Rock", Proceedings Second Midwest Conference on Solid Mechanics, Purdue University, 1955, pp. 178-192.

(36) T. L. Watson, "Granites of Georgia", State of Georgia Geological Reports, no. 9A, pp. 114-117.

(37) N. Webster, Webster's New World Dictionary of the American Language, College Edition, World Publishing Company, Cleveland, 1957, p. 578.

(38) A. W. Skempton," Effective Stress in Soils, Concrete and Rocks", Pore Pressure and Suction in Soils, Butterworths, London, 1961, pp. 4-16.

OTHER REFERENCES

Bridgman, P. W., "Some Implications for Geophysics of High Pressure Phenomena", Bulletin of the Geological Society of America. vol. 62, 1951, pp. 533-536.

Dana, J. D. Manual of Mineralogy, 17th ed., John Wiley and Sons, London, 1959, 609 pp.

Donath, F. A. "Experimental Study of Shear Failure in Anisotropic Rocks", Bulletin of the Geological Society of America, vol. 72, no. 6, 1961, pp. 985-989.

Frocht, M. M., Strength of Materials, Ronald Press Company, New York, 1951, pp. 106-155.

Kirkpatrick, W. M., "The Condition of Failure for Sands", Proceedings of the Fourth International Conference on Soil Mechanics and Foundation Engineering, London, 1957, pp. 172-177.

Newmark, N. M., "Failure Hypothesis for Soils", ASCE Research Conference on Shear Strength of Cohesive Soils, Boulder, Colorado, 1960, pp. 17-32.

Seed, H. B.; Mitchell, J. K.; and Chan, C. K., "The Strength of Compacted Cohesive Soils", ASCE Research Conference on Shear Strength of Cohesive Soils, Boulder, Colorado, 1960, pp. 877-964.

Sowers, G. F., Earth and Rockfill Dam Engineering, Asia Publishing House, New York, 1962, 283 pp.

Sowers, G. F. and Sowers, G. B., Introductory Soil Mechanics and Foundations, 2nd ed., The Macmillan Company, New York, 1961, 385 pp.

Taylor, D. W., Fundamentals of Soil Mechanics, John Wiley and Sons, Inc., New York, 1948, 700 pp.

Terzaghi, K., Theoretical Soil Mechanics, John Wiley and Sons, Inc. New York, 1959, 510 pp.

Timoshenko, S. and Goodier, J. N., Theory of Elasticity, 2nd ed., McGraw-Hill Book Company, New York, 1951.

Topping, A. D., "Rock Strength: The Conditions of Failure", World Oil, vol. 141, 1955, pp. 109-117.

Tschebotarioff, G. P., Soil Mechanics, Foundations, and Earth Structures, McGraw-Hill Book Company, New York, 1951, pp. 120-125.

Whitman, R. V., "Some Considerations and Data Regarding the Shear Strength of Clays", ASCE Research Conference on the Shear Strength of Cohesive Soils, Boulder, Colorado, 1960, pp. 581-614.

Wyerker, R. G., "Measuring the Tensile Strength of Rocks", Mining Engineering, vol. 7, no. 2, 1955, p. 157.

VITA

Arnold Edward Schwartz was born December 15, 1935, in Rochester, New York. He was graduated from the Aquinas Institute, Rochester, New York in 1953; thereupon he entered the Civil Engineering program at the University of Notre Dame, Notre Dame, Indiana. He received the degree Bachelor of Science in Civil Engineering in 1958 and Master of Science in Civil Engineering in 1960 from Notre Dame. Thereafter, he entered the Georgia Institute of Technology as a candidate for the degree Doctor of Philosophy in the School of Civil Engineering. Mr. Schwartz has held the position of Graduate Teaching Assistant throughout his graduate study and in 1962 was awarded a Ford Foundation Fellowship. He has been employed by the State of New York; Clyde Williams, Associates, South Bend, Indiana; and the Engineering Experiment Station, Georgia Institute of Technology, Atlanta, Georgia. Upon completion of graduate studies, Mr. Schwartz will assume the duties of Assistant Professor of Civil Engineering at Clemson College, Clemson, South Carolina.